Click here to view PowerPoint presentation; Press Esc to exit

Net Shape Manufacturing of Aeroengine Components

Xinhua Wu

IRC in Materials, the University of Birmingham, Edgbaston, B15 2TT

e-mail: X.Wu.1@bham.ac.uk

ABSTRACT

Direct laser fabrication (DLF) and Net shape HIPping are two net shape manufacturing technologies which are being studied in the IRC. The direct laser fabrication technique can produce 3-D components from their CAD files from metal powder and using a laser, the movement of which follows the paths defined by the CAD file whilst powder is being injected into its focal point. The correlation between the thermal history and microstructure will be illustrated. Some demonstration pieces will be shown.

Net Shape HIPping (Hot Isostatic Pressing) is a technology to manufacture large components from powder to final shape component in one step. This technology uses cheap mild steel as tooling/mould material, which is filled with metal powder, followed by HIPping to consolidate the powder. A net shape component is subsequently obtained after removing of the tooling through machining/pickling. The geometry of the tooling/mould is designed through sophisticated computer modelling, taking into account the shrinkage during powder consolidation, mild steel deformation etc. so that the final geometry of the component is exactly that required after removing of the tooling. The mechanical properties obtained using this technique are similar to those in wrought components. Examples of the application of this net shape HIPping technology in manufacturing demonstrator components will be described.

1.   DIRECT LASER FABRICATION

1.1   Introduction

Direct Laser Fabrication(DLF) is one of the acronyms for laser additive manufacturing, where a laser is used as a heat source and metal powder is injected into the laser focal point and the movement of the laser is defined by the CAD file of a component. A 3D component is thus built layer by layer from the CAD file directly without using any mould.

Previous research shows that many variables in this process affect the material properties and the microstructure of the resulting part, such as laser scanning speed, laser power and powder feed rate. A number of previous efforts have been undertaken to establish the relationship between process parameters and the microstructure of deposits and it was found that the effects of each parameter could not be isolated because they are not independent [1, 2]. In order to achieve a better understanding of the effects of processing parameters on microstructures of DLFed samples, it is paramount to understand the temperature behavior/history of samples during fabrication. In this study, a 3D transient finite element model for direct laser fabrication has been developed by using a commercial Finite Element tool ABAQUS. Ti-6Al-4V is used as an experimental material since it is an important aerospace

Report Documentation Page

Form Approved
OMB No. 0704-0188

Public reporting burden for the collection of information is estimated to average 1 hour per response, including the time for reviewing instructions, searching existing data sources, gathering and maintaining the data needed, and completing and reviewing the collection of information. Send comments regarding this burden estimate or any other aspect of this collection of information, including suggestions for reducing this burden, to Washington Headquarters Services, Directorate for Information Operations and Reports, 1215 Jefferson Davis Highway, Suite 1204, Arlington VA 22202-4302. Respondents should be aware that notwithstanding any other provision of law, no person shall be subject to a penalty for failing to comply with a collection of information if it does not display a currently valid OMB control number.

1. REPORT DATE **MAY 2006**	2. REPORT TYPE **N/A**	3. DATES COVERED **-**

4. TITLE AND SUBTITLE **Net Shape Manufacturing of Aeroengine Components**	5a. CONTRACT NUMBER
	5b. GRANT NUMBER
	5c. PROGRAM ELEMENT NUMBER
6. AUTHOR(S)	5d. PROJECT NUMBER
	5e. TASK NUMBER
	5f. WORK UNIT NUMBER
7. PERFORMING ORGANIZATION NAME(S) AND ADDRESS(ES) **IRC in Materials, the University of Birmingham, Edgbaston, B15 2TT**	8. PERFORMING ORGANIZATION REPORT NUMBER
9. SPONSORING/MONITORING AGENCY NAME(S) AND ADDRESS(ES)	10. SPONSOR/MONITOR'S ACRONYM(S)
	11. SPONSOR/MONITOR'S REPORT NUMBER(S)

12. DISTRIBUTION/AVAILABILITY STATEMENT
Approved for public release, distribution unlimited

13. SUPPLEMENTARY NOTES
See also ADM202748. Cost Effective Manufacture via Net Shape Processing (Rentabilite de fabrication par un traitement de finition immediate), The original document contains color images.

14. ABSTRACT

15. SUBJECT TERMS

16. SECURITY CLASSIFICATION OF:			17. LIMITATION OF ABSTRACT	18. NUMBER OF PAGES	19a. NAME OF RESPONSIBLE PERSON
a. REPORT **unclassified**	b. ABSTRACT **unclassified**	c. THIS PAGE **unclassified**	**SAR**	**48**	

Standard Form 298 (Rev. 8-98)
Prescribed by ANSI Std Z39-18

material and some previous research on DLF has been carried out on this material and also because of the availability of the material's physical and metallurgical properties [1, 2]. This paper presents the modelling results on the effects of the location and laser scanning speed on temperature profile/history of the deposited Ti-6Al-4V thin-wall sample. The simulation results have been correlated with the microstructure and the size of α and β laths of this α+β alloy.

1.2   Finite Element Model

In the process of producing the thin-wall shaped sample by DLF, the sample absorbs energy from laser heating and loses energy via conduction, convection, radiation. For Ti-6Al-4V the sample also absorbs energy during material melting or during α to β transformation and releases energy during material solidification or β to α transformation. The general purpose, finite element package ABAQUS standard (version 6.4) was used for the calculation of the thermal mathematical model. The sample configuration is shown in figure 1. The thin-wall sample has a width of 20mm (X axis), a thickness of 2mm (Y axis), a layer increment of 0.3mm and a final height of 20.1mm (Z axis). The size of the substrate is 48×8×24mm.

In the ABAQUS model, the heat source was simplified as a moving surface heat flux assigned on the top surface of elements according to time and laser scanning speed. Heat is transferred to the bottom substrate via conduction. The rest of the surface loses heat to the surrounding area via radiation and convection. Considering that the laser beam is always centred on the thin-wall sample along the X axis as shown in figure 1, the sample has a symmetrical temperature distribution about the centre in the Y direction. The symmetrical boundary can be realized by setting the boundary condition as insulated since there would be no heat flow across the boundary. The thin-wall geometry has 67 layers and 1340 3-dimensional 8 node elements (DC3D8) [4]. The element size of the model is 1×1×0.3mm. The thin-wall part is of finer mesh than the substrate region for better accuracy of the temperature results in the thin-wall. All the models in this study have identical dimensions. The temperature-dependent thermal material properties, thermal conductivity and heat capacity used in this study have been taken from the literature [5].
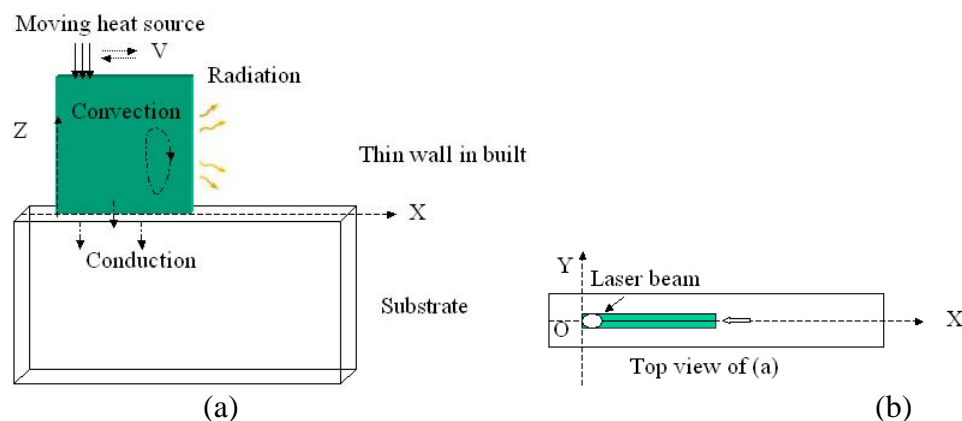

Figure 1: (a) A schematic illustration of a DLFed thin-wall sample build; (b) a top view showing the molten pool position is symmetric along the X-axis as shown by the arrow.

1.3   Experimental

A series of thin-wall shaped samples with 20×2×20.1mm dimensions were produced using DLF with a single pass laser in an argon atmosphere with $O_2 < 20$ppm. Ti-6Al-4V powder with particle size between 100-250µm was used in this study. A 1750W CO_2 laser unit was used in the experiment. The laser processing parameters used are laser powers of 432W and 516W, laser scanning speed of 300, 400, 600 and 900mm/min and powder feed rates of 9 and 18g/min. The front surface of the samples was examined using both optical microscopy and scanning electron microscopy (SEM). Four K-type thermocouples were welded on the Ti-6Al-4V substrate prior to the deposition process. Temperature measurements were synchronized with sample fabrication by inserting three W-type thermocouples into the samples during the build. These were inserted manually into pre-selected positions and the actual position could be defined when the build was completed. A data logging system from National Instruments was used to collect information of temperature against time for four K-type and three W-type thermocouples simultaneously. SEM examinations were conducted using a Jeol 6060.

1.4   Results and discussion

1.4.1   Comparison of temperatures between the measurements and predictions

Figure 2a shows temperature measurements and predictions for two locations on the DLFed thin-wall sample (W1, W2) and one location on the substrate (K1). The letters W and K indicate the type of the thermocouple used. Figure 2b shows the positions of W1, W2 and K1. The data from W1, W2 show the characteristic temperature history of a DLFed thin-wall sample. The sample from which the data shown in figure 2a was obtained was fabricated with a 516W laser power, 400mm/min laser scanning speed and 9g/min powder feed rate. Each temperature peak represents the thermocouple

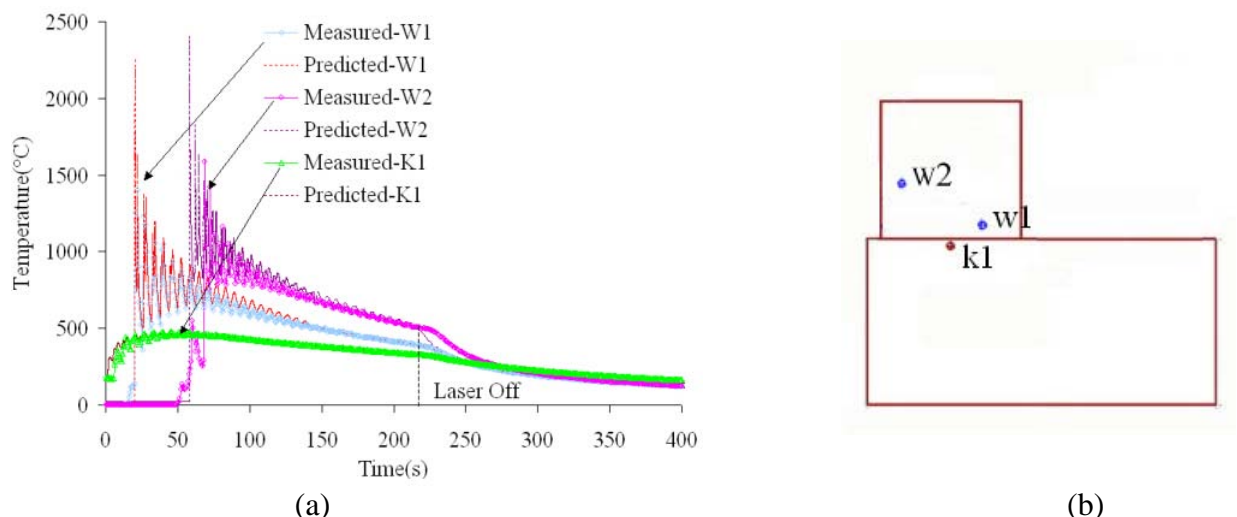| (a) | (b) |

Figure 2: (a) Comparison of temperatures between predictions and measurements on the DLFed thin-wall sample (W1, W2) and substrate (K1). The measured and the predicted thermal profiles overlap with each other and are very difficult to separate; (b) a schematic illustration showing the locations of K and W-type thermocouples on the substrate and the DLFed thin-wall sample.

response as the laser passes over the thermocouple. The rapid decrease of temperature from the peaks to the troughs reflects the movement of the heat source moving away from the thermocouple along the X-axis. The thermal excursion decays when either the energy source moves away from thermocouple during fabrication of an individual layer or when subsequent layers are deposited. From comparison of predicted and measured temperature history on the sample and the substrate, we can see the main trends match fairly well. In fact, the measured and the predicted thermal profiles overlap with each other and are very difficult to separate.

1.4.2   *Phase transformation of Ti-6Al-4V during cooling*

It has been reported previously that the cooling rate from the β phase region to a temperature below the β/(α+β) transus, 980°C [6, 7], defines the nature of the β phase, whether it will be martensite (α′) (if cooling rate > about 410°C/s [8]) or diffusion-controlled Widmanstätten structure (if the cooling rate is < 20°C/s).

The cooling rate and the time spent at temperatures below, but close to, the β/(α+β) transus temperature, (e.g. between 600-980°C, especially between 800-980°C when α laths can grow rapidly) would be expected to affect the size of α laths in a basketweave microstructure. The temperatures reached during cooling will define the fraction of martensite formed (the martensite finish temperature is below room temperature) and the fraction of α and transformed β. During subsequent excursions above 980°C the martensite and any transformed β will be unstable and may partially transform back to β. This could re-transform to martensite if subsequently cooled to a low enough temperature rapidly enough, or re-precipitate as α. On that basis the precise microstructures expected are difficult to predict, but an attempt to do this for DLFed samples is made below.

1.4.3   *The influence of location in a sample on microstructure and thermal history*

Typical microstructures obtained in DLF are shown in figure 3 where some very long, laths have been identified using X-ray and TEM as martensite. It is noted that the amount of martensite which protrude from the surface gradually reduces with the sample height and almost completely disappears 14mm away from the bottom, figure 3c. It is also noted that there is a larger amount of martensite at the bottom and at the very top, comparing figures 3a, e with figures 3b to d.

In figure 4, the temperature-time (T-t) curves show the temperature history prediction at the bottom, 3mm away from the bottom, centre, near the top and very top of a DLFed sample. In these five temperature history curves, the temperature drops down smoothly from the peak temperatures and the cooling rate across the β transus has been found to be ~7x10^{4}°C/S through modelling. It can be seen from figure 4 that with increase of sample height the duration of time spent in the α+β region and the temperatures experienced both increase below 9mm, as indicated by the first two curves on the left. Hence larger α laths are expected with increase of height, which is evident, comparing figure 3b with 3a. At a height of 6mm away from top the temperature decreases slowly across the β transus which means there should be no martensite at this location, which is consistent with the microstructure shown in figure 3c. At the top of the sample the cooling rate is again about 10^{4}°C/s as shown by the right curve on figure 4 and significant martensite is thus expected as is confirmed by figure 3e.
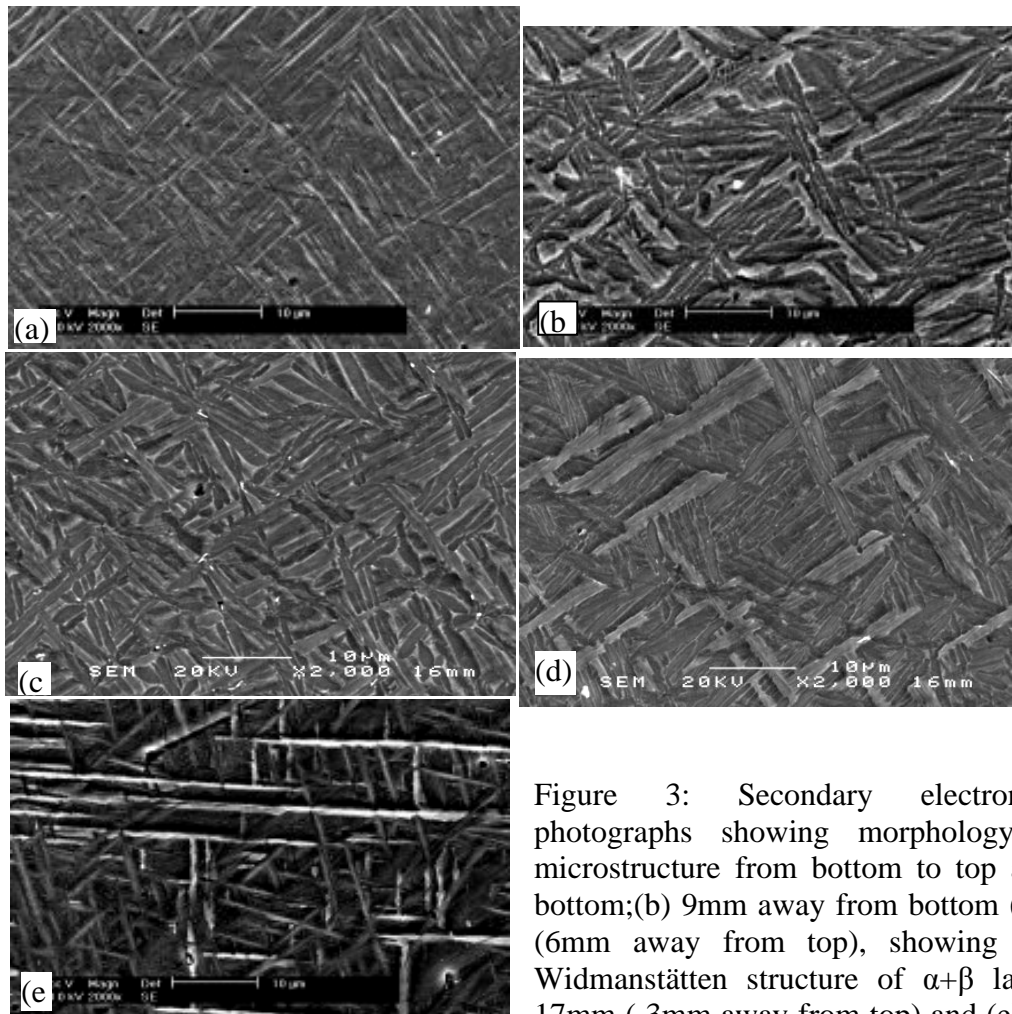
Figure 3: Secondary electron SEM photographs showing morphology of the microstructure from bottom to top at (a) the bottom;(b) 9mm away from bottom (c) 14mm (6mm away from top), showing complete Widmanstätten structure of α+β laths ; (d) 17mm (3mm away from top) and (e) the very top, The protruding long laths/plates are martensite. Laser process condition: powder feed rate 18g/min, laser power 432 W and laser scanning speed 600mm/min.
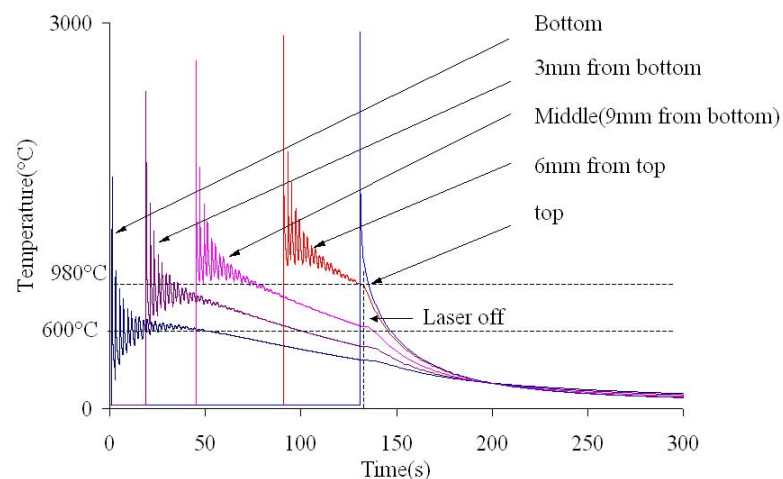

Figure 4: Temperature histories at a series of locations along the height of the sample. The curves from left to right in turn represent location: (1) bottom; (2) 3mm away from the bottom; (3) 9mm away from the bottom; (4) 14mm away from bottom (6mm away from top) and (5) the very top of the DLFed build at laser scan speed 600 mm/min, laser power 432W and powder feed rate 18g/min.

1.5   Summary
A 3-D Finite Element Model has been used to model the thermal profiles of a Ti64 sample during its fabrication using DLF process and a good match has been obtained between the predicted and measured thermal histories. The thermal profiles at various locations are also consistent with the microstructures obtained.

2. NET SHAPE HIPPING

2.1   Introduction

Net shape HIPping is an advanced manufacturing technology which uses a cheap mild steel mould, filled with Ti or Ni alloy powder, which is sealed then outgassed and finally, Hot-Isostatically-Pressed (HIPped). The mould is designed using sophisticated computer modelling, taking into account material deformation, powder densification at high temperature and high pressure during HIPping. If the computer modelling is correct the component should have defined dimension after the mild steel mould is removed mechanically or through pickling. This technique is very useful for making large or medium sized complex components.

2.2   Experimental

The Ti6Al4V (Ti64) powder used is commercial PREP(plasma rotating electrode process) powder supplied by Advanced P Metal, USA. The powder particle size ranges from 50 to 350μm. The oxygen content in the ingot feedstock for atomisation is about 1600ppm. The powder was filled into mild steel cans, then outgassed for a range of times. The HIPping was carried out at 930°C/4h at 150MPa. A small cylindrical casing was designed using modelling software provided by LNT, Russia and mild steel was used as tooling material, which was removed through pickling after the HIPping. The geometries of the manufactured small component were measured by a Co-ordinate Measurement Machine (CMM) and compared with the predictions. In addition a tensile sample with as-HIPped surface has also been manufactured. Tensile tests were carried out using a Zwick machine at a strain rate of ~$10^{-4}s^{-1}$. Some materials were cut out for oxygen analysis

2.3   Results and discussion

The tensile properties and oxygen content for samples which have been outgassed for a range of times, are shown in Table 1. It can be seen that the duration of outgassing for Ti64 has little effect on the tensile properties, where the yield stress is ~880MPa, UTS ~ 960MPa and ductility ~22%, which means that a 4h outgassing is sufficient for such size of samples and excessively long outgassing appears not to further remove oxygen significantly. For the sample with an as-HIPped surface there is ~50MPa reduction in strength and ~3% reduction in ductility. This is possibly introduced by the undulation on the as-HIPped surface when mild steel tooling is used, figure 6(a). Ti64 is stronger than mild steel at the HIPping temperature of 930°C, consequently Ti64 powder at the surface can penetrate into the mild steel capsule, leaving particle-shaped undulations on a pickled surface. Nevertheless the overall property of HIPped Ti64 with as-HIPped surface is still comparable to that of commercial ring-rolled Ti64 which has a

yield stress of between 830-960MPa, UTS 900-1040MPa and ductility of 8-12%[6]. Examinations of fracture surfaces have shown that HIPped Ti64 failed in a normal ductile manner with either machined or as-HIPped surface condition. Figure 6(b) shows the fracture surface of the sample with as-HIPped surface and no abnormal characteristic has been observed at the surface. It appears that despite the small reduction of property caused by the undulations at the sample surface the fracture behaviour remains similar to the as-machined.

Table 1: Showing tensile properties of HIPped Ti64 with a range of outgassing times

Outgassing time(h)	Oxygen (wt%)	0.2% proof stress (MPa)	UTS (MPa)	Elongation (%)
4.0	0.17	879	967	23
5.0	0.18	878	968	24
5.6	0.17	881	971	20
16.4	0.19	876	967	21
16.7	0.18	879	968	23
20.6	0.17	877	992	22
25.0	0.17	879	967	23
12 (as-HIPped surface)	*-*	*850*	*920*	*19*
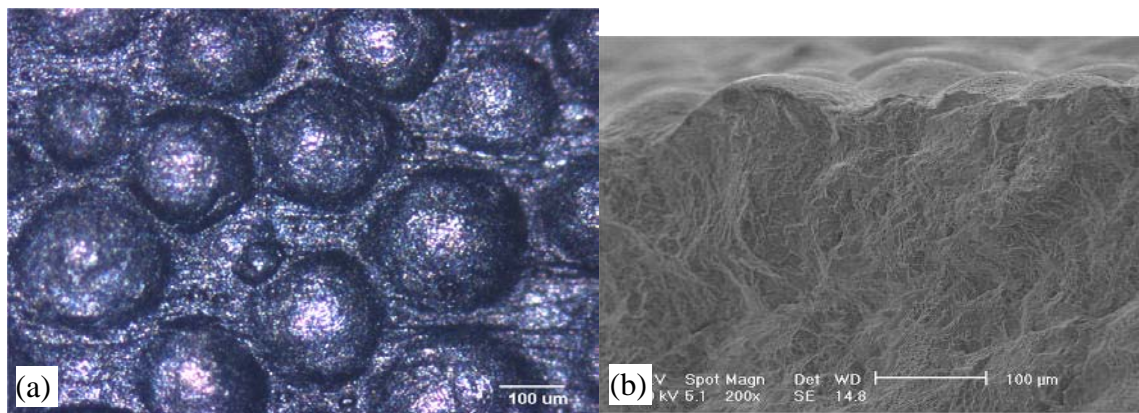
Figure 6: Showing (a) as-HIPped surface morphology of a net shaped tensile sample produced using mild steel tooling and (b) tensile fracture surface of HIPped Ti64 with as- HIPped surface

A demonstrator component of Ti64 has been modelled, designed and manufactured using net shape HIPping as shown in figure 7. The thinnest section in this component is about 0.4mm (note that the powder particle size used in this case is 50-150μm). The cross-section dimensions at various locations have been measured and compared with computer predicted (target) dimensions.

Table 2 and figure 8 show the results of inner dimensions at 10 locations. In general, the prediction of final consolidated shape of the main cylindrical body compares reasonably well with the HIPped component (by CMM measurements), as indicated in

table 2. A reasonably good match is especially shown in the lower part of the thin cylinder wall. However in the top part of the cylinder wall, the side where the filling tubes are welded, some changes in wall thickness and inclinations are apparent. The predictions and measurements for positions along the cylinder height are also in good agreement for each of the ring and boss features.
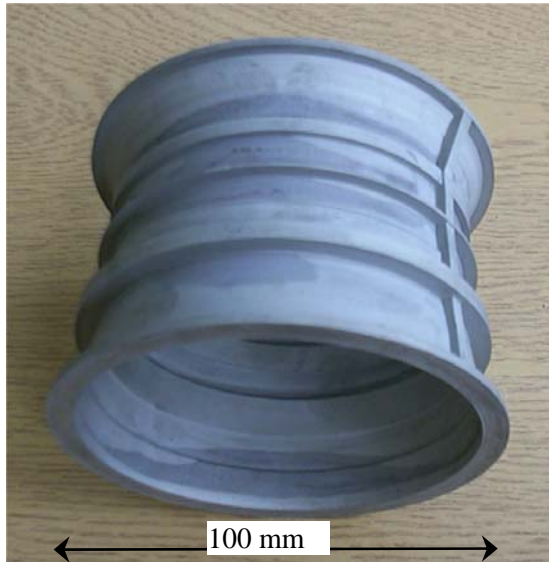
Figure 7: Showing the net-shape-HIPped mini Ti64 casing.

Table 2: Showing the comparison of dimensions between the computer predicted and measured

	Target (mm)	Actual (mm)	Discrepancy (mm)
i	45.59	-	-
ii	40.35	40.25	0.10
iii	41.16	40.94	0.22
iv	38.18	38.18	-
v	39.98	40.07	-0.09
vi	38.43	38.31	0.12
vii	40.97	40.88	0.09
viii	39.94	39.98	-0.04
ix	41.68	41.70	-0.02
x	43.40	43.41	-0.01
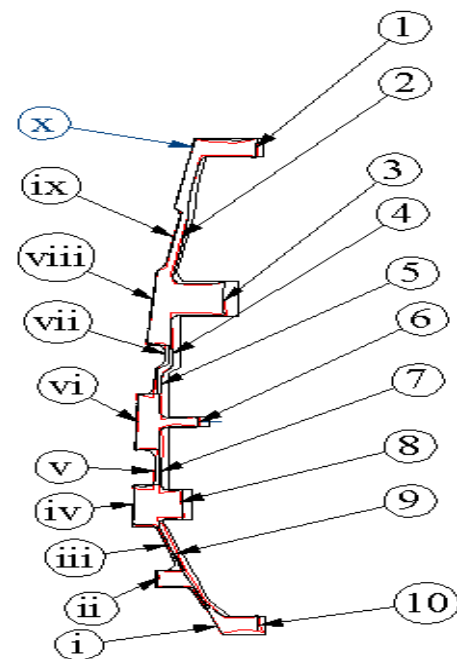
Figure 8: Showing the locations where measurements have been carried out. The inner dimensions at location i to x are shown in table 2.

2.4 Summary

The mechanical properties of the HIPped Ti64 either with machined or as-HIPped surface are better than those of the ring-rolled. As-HIPped surface introduces small reduction in tensile property.

A demonstrator mini-casing manufactured using net shape HIPping shows very good integrity and the discrepancy between the predicted and the measured dimension is within 0.1mm at most locations.

3. ACKNOWLEDGEMENTS

4. REFERENCES

[1] X. Wu, R. Sharman, J. Mei, and W. Voice, Direct laser fabrication and microstructure of a burn-resistant Ti alloy, Materials & Design. Vol. 23, Issue 3 (2002), p. 239-247.

[2] X. Wu, J. Liang, J. Mei, C. Mitchell, P. S. Goodwin and W. Voice, Microstructures of laser-deposited Ti–6Al–4V, Materials & Design, Vol.25, Issue 2 (2004), p.137-144.

[3] X. Wu, R. Sharman, J. Mei and W. Voice, Microstructure and properties of a laser fabricated burn-resistant Ti alloy, Materials & Design, Vol.25, Issue 2 (2004), p.103-109.

[4] ABAQUS theory manual version 6.4. Section 2.11.1.

[5] K. C. Mills, Recommended values of thermo-physical properties for selected commercial alloys, (NPL) (2002), p. 211-217.

[6] R. Boyer, G. Welsch and E. Collings, Material properties handbook: titanium alloys, 1994, ASM international, U.S.A, p.488.

[7] Z. Zwicker, Metallkde. (1956), Bd.47, Heft 8, p. 535-548.

[8] T. Ahmed and H. Rack, Phase transformations during cooling in $\alpha+\beta$ titanium alloys, Materials Science & Engineering (1998), A243, p. 206-211.

MEETING DISCUSSION – PAPER NO: 5

Author: X. Wu

Discusser: D. Dicus

Question: Given the critical impact of cooling rate that you showed for DLF of Ti-6-4, would you expect to require a process control system for cooling rate?

Response: Yes. The control system is expected to be incorporated into the new system which is to be purchased soon.

Discusser: J. Savoie

Question: How can the influence of deposition parameters on residual stresses.be minimized? Using FE modeling?

Response: By changing the laser scan path. Can be modeled using FE.

Discusser: C. Bampton

Question: Why is the residual stress in HIP'd Ti with mild steel insert so low?

Response: There is sliding between Ti and steel tooling hence low residual stress.

Discusser: M. Hicks

Question: Why do we see equiaxed microstructures in some Ti alloys which have been laser deposited (e.g. burn resistant Ti) and columnar in others (e.g. Ti-6-4)?

Response: It is affected by the liquidus/solidus gap and slope. Some Ti alloys (e.g. burn resistant Ti) have very small gap, hence the under-cool required for nucleation is very small, which leads to easy nucleation, thus equiaxed grains.

Net Shape Manufacturing of Aeroengine Components

Xinhua Wu

IRC in Materials
The University of Birmingham

Contents

- Net Shape HIPping

  – *Demo and mechanical property*

- Direct Laser Fabrication

  – *Computer modelling of thermal history*

  – *Correlation between thermal profiles and microstructure/residual stress*

Net Shape HIPping

- Using mild steel tooling

- PREP Ti6Al4V powder, 50-350μm

Ti-6Al-4V powder demos manufactured in Bham using Net Shape HIPping technique

1/7 V2500 casing demo

(Thinnest wall section = 0.4mm)

Comparison of the Inner Radius between the Prediction and the HIPped Casing

	Target (mm)	Actual (mm)	Discrepancy (mm)
i	45.59	-	-
ii	40.35	40.25	0.10
iii	41.16	40.94	0.22
iv	38.18	38.18	-
v	39.98	40.07	-0.09
vi	38.43	38.31	0.12
vii	40.97	40.88	0.09
viii	39.94	39.98	-0.04
ix	41.68	41.70	-0.02
x	43.40	43.41	-0.01

News

A 3D Laser measurement system is now installed in the IRC

1. Accuracy: 10μm
2. Measurement size:
   Φ 1m, Height 600mm
3. Provide CAD files
   after measurements

x10-6m

300μm

150μm

0

Interdisciplinary **R**esearch **C**entre **in Materials for High Performance Applications**

THE UNIVERSITY OF BIRMINGHAM
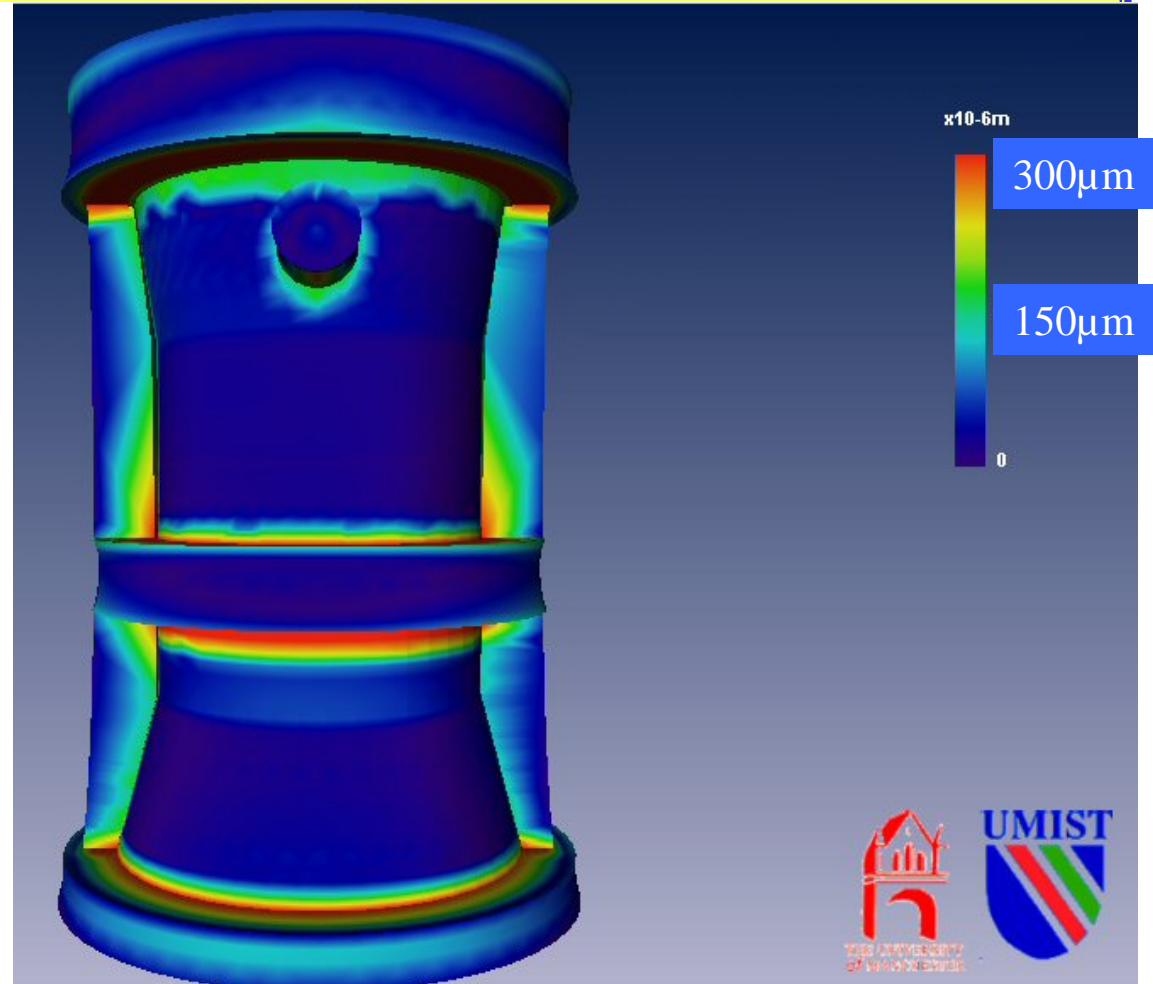
Tensile properties of HIPped Ti6Al4V (machined tensile samples and as-HIPped tensile sample)

Outgassing time(h)	Oxygen (wt%)	0.2% proof stress (MPa)	UTS (MPa)	Elongation (%)
4.0	0.17	879	967	23
5.0	0.18	878	968	24
16.4	0.19	876	967	21
20.6	0.17	877	992	22
25.0	0.17	879	967	23
12 (As-HIPped surface)	-	*850*	*920*	*19*

Design Property   **830-960**   **900-1040**   **8-12**

HIPped Ti6Al4V fracture toughness: 20°C

Specimen	K_{IC} (MNm$^{-3/2}$)
1	94.0
2	96.5
3	92.5

➢ Compact tension (CT) specimens

➢ BS 7448-1 (1991)

➢ Type 1 load vs displacement

➢ Plane strain criteria confirmed

➢ Good consistency

➢ K_{IC} values relatively high

Forged Ti6Al4V K_{IC}=55 MNm$^{-3/2}$

Influence of surface condition on fatigue limit (4-point bending)

Interdisciplinary
Research **C**entre
in Materials for High
Performance Applications

THE UNIVERSITY
OF BIRMINGHAM
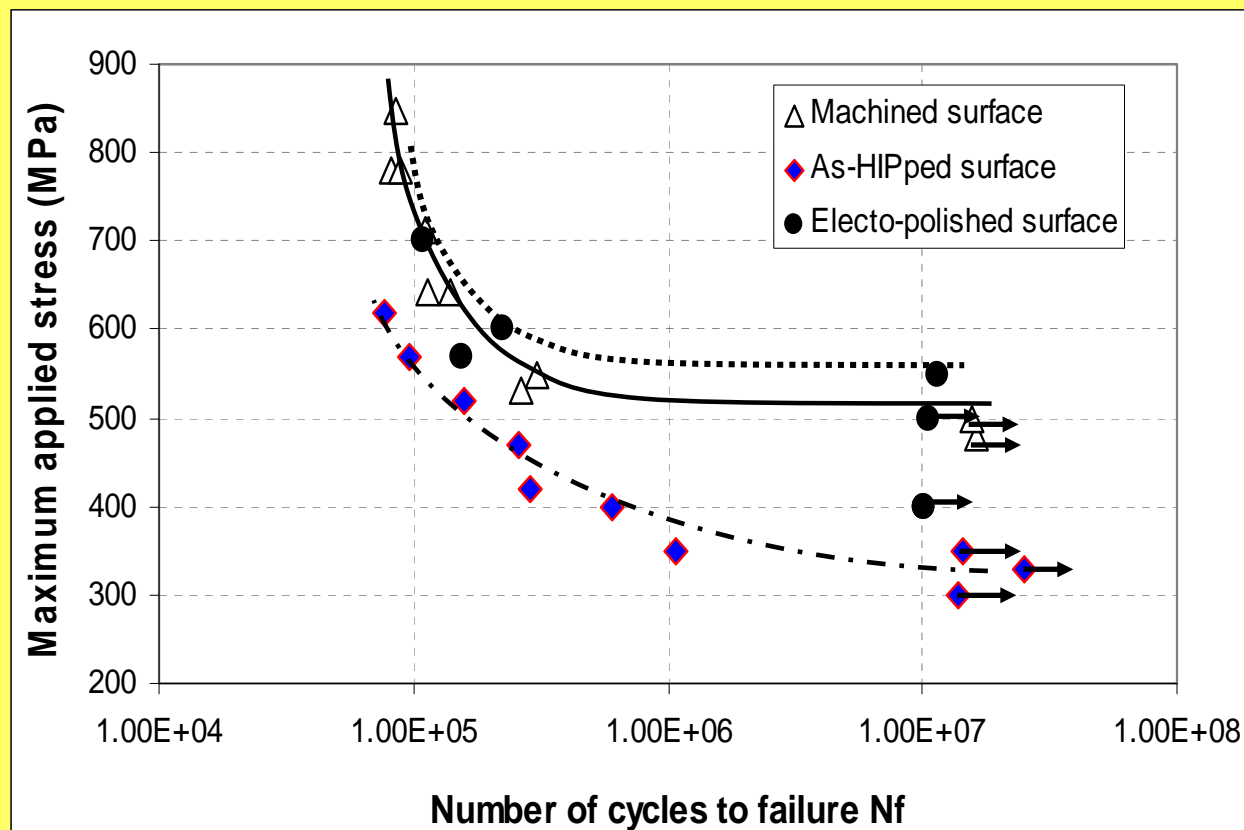
Surface topographs of fatigue samples

Machined
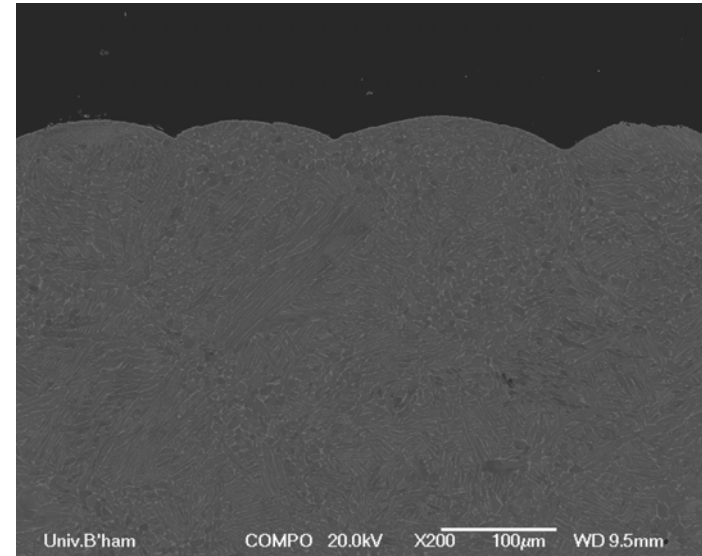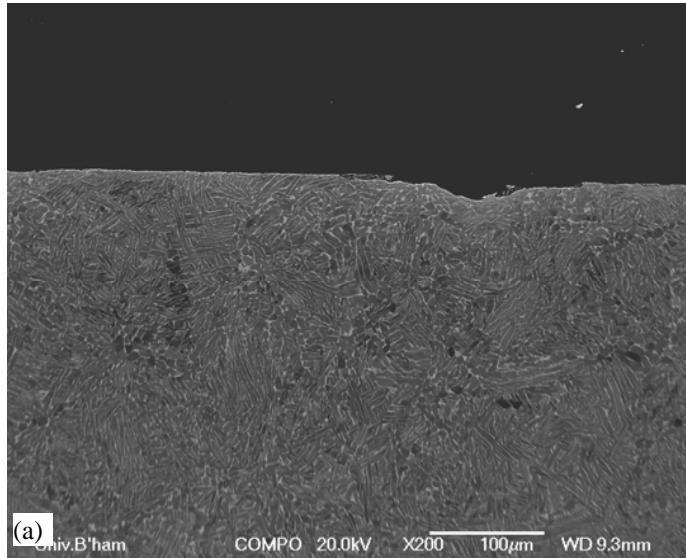
As-HIPped

Electro-polished
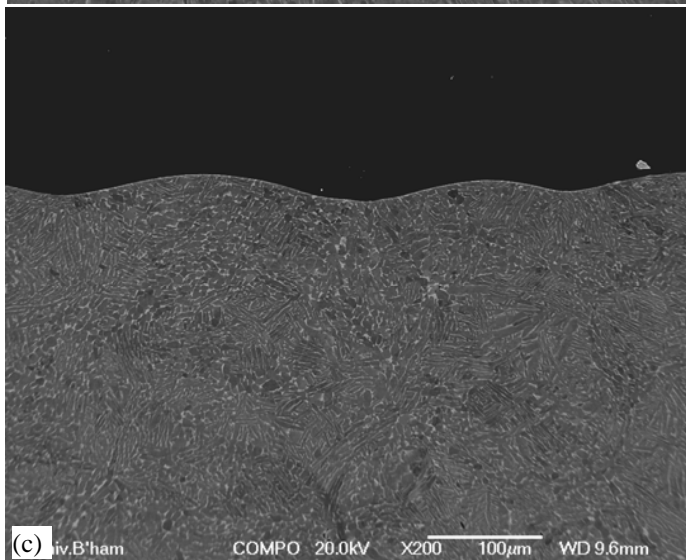
Solution: 60% Methanol
        35% 1-Butanol
        5% $HClO_4$
Temp: -35°C (Methanol+Lq N2)
Holding time: 50 min
Current: 0.8~1A

Thermal residual stress measurement in HIPped Ti64

Set-up on beam line ID31 for measuring out-of-plane strain in the near surface region of a cylindrical sample
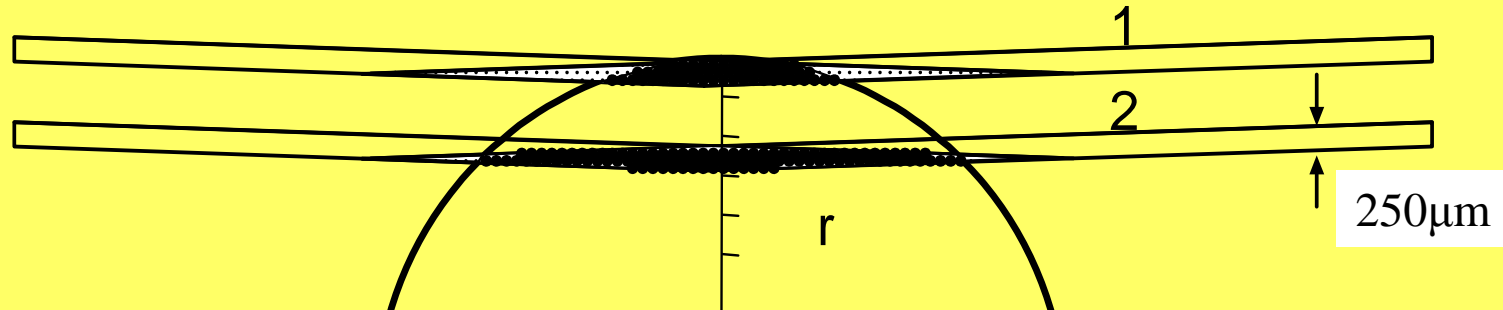
Beam 1 indicates a measurement point right at the surface

Beam 2 indicates a measurement point further into the sample

Thermal residual stress in HIPped Ti6Al4V measured using synchrotron
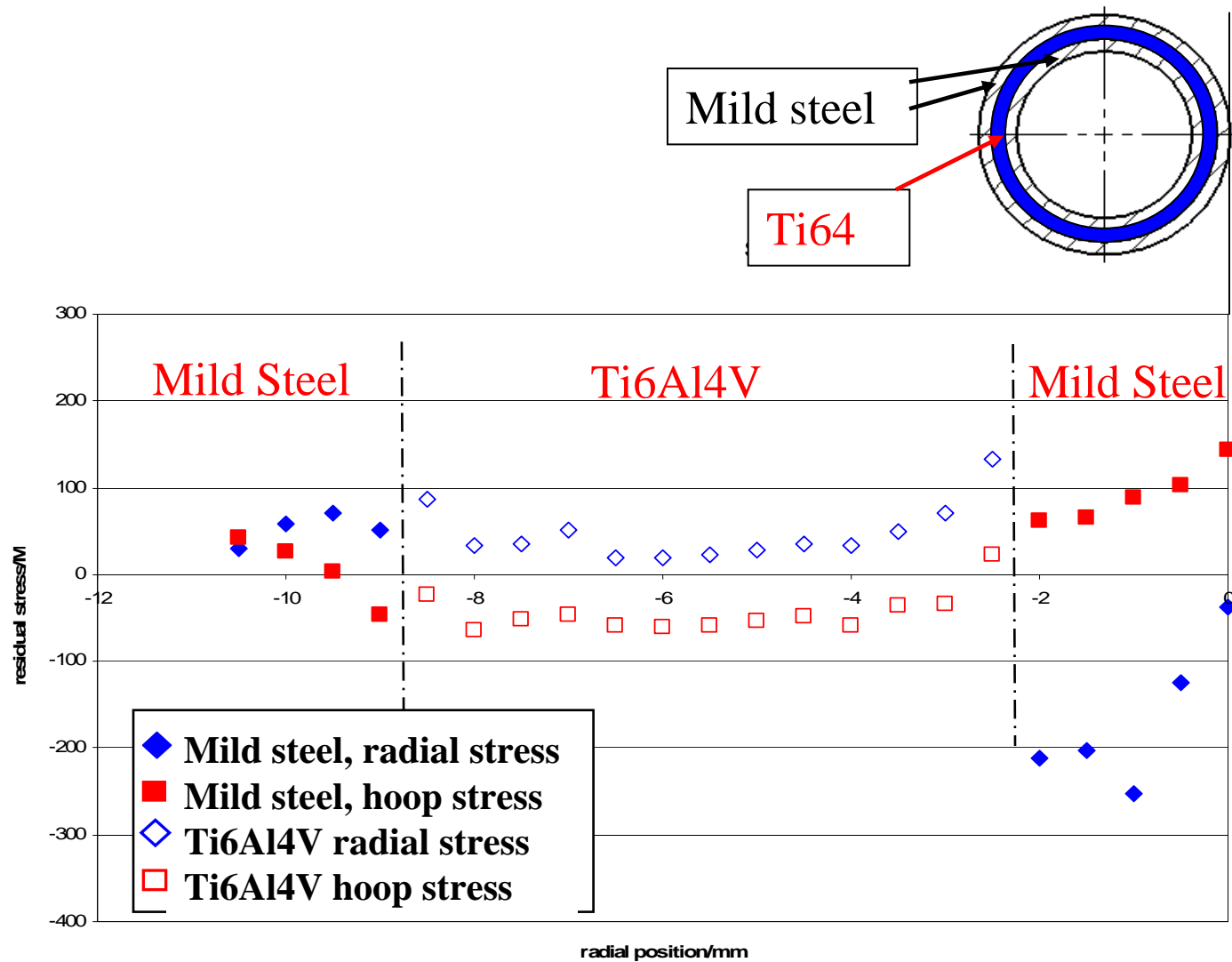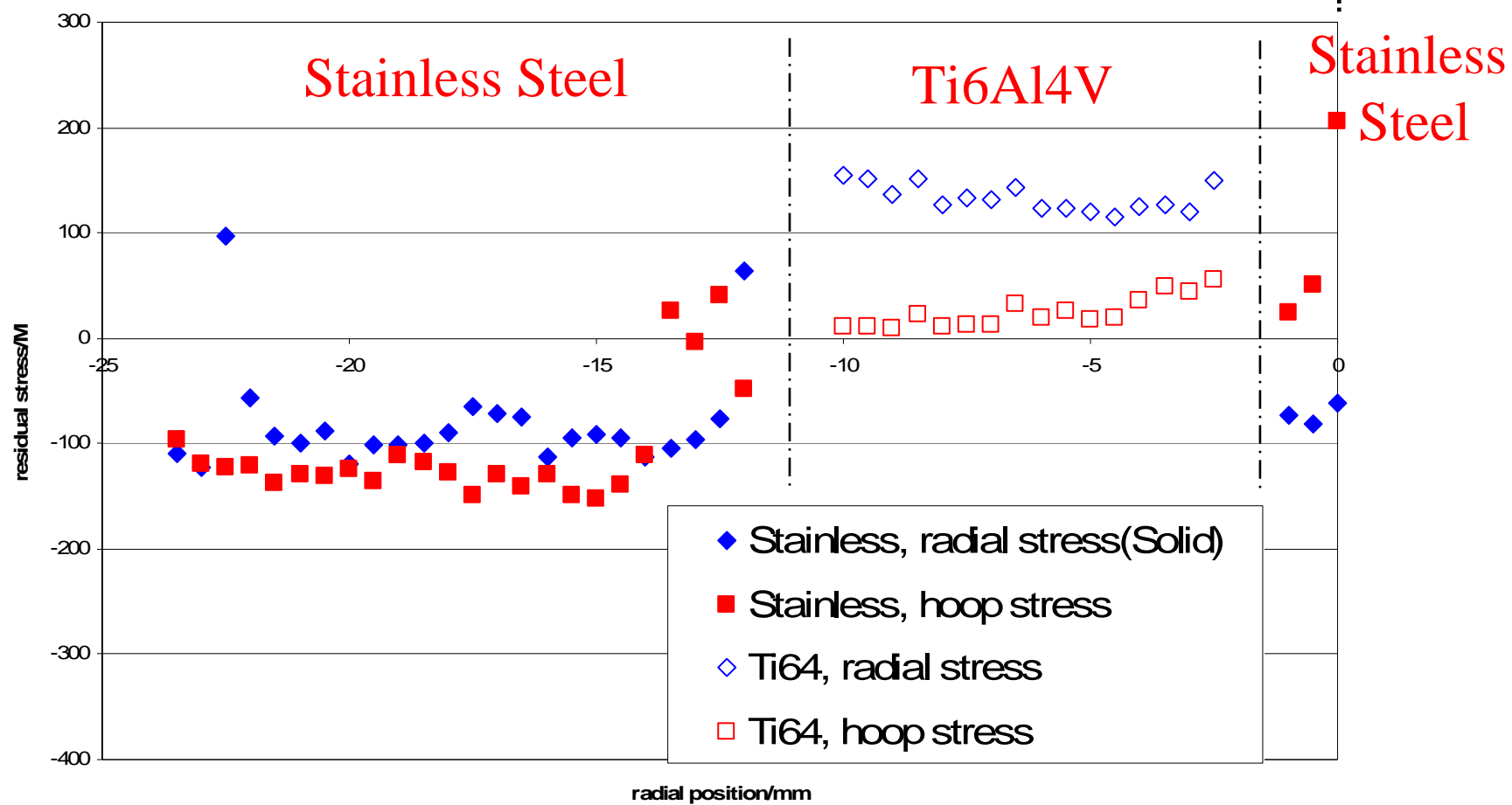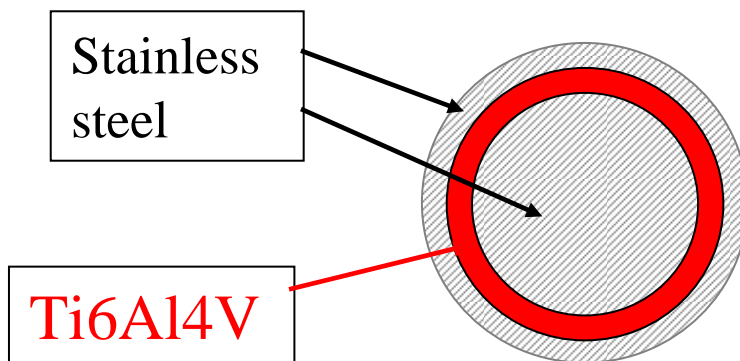
Summary

- Net shape HIPping produces good dimension discrepancy

- The HIPped property is as good as forged

- The residual stress in the component is negligible

Parts laser fabricated
from Ti alloys

08.07.2005

Parts laser fabricated
from Ni alloys

Ti6Al4V to BuRTi

Ti6Al4V to (TiC+Ti6Al4V)

100 um

TiC +Ti6Al4V

Interface   Ti6Al4V

Univ.B'ham   SEI   20.0kV   X500   10µm   WD 9.7mm
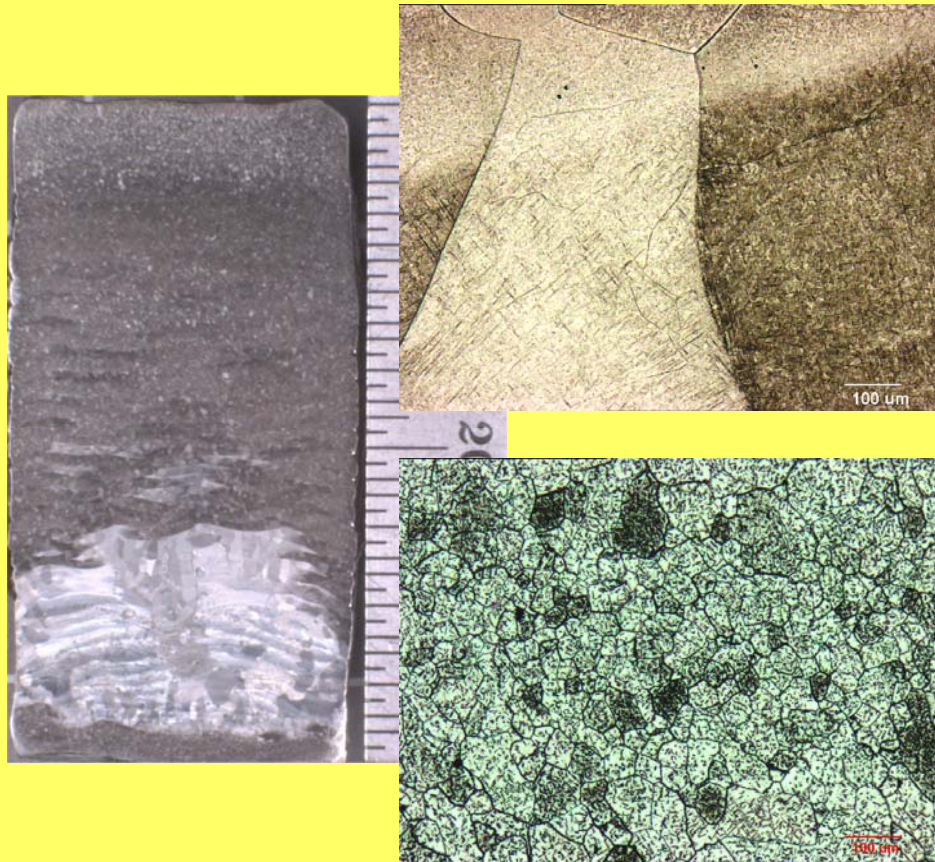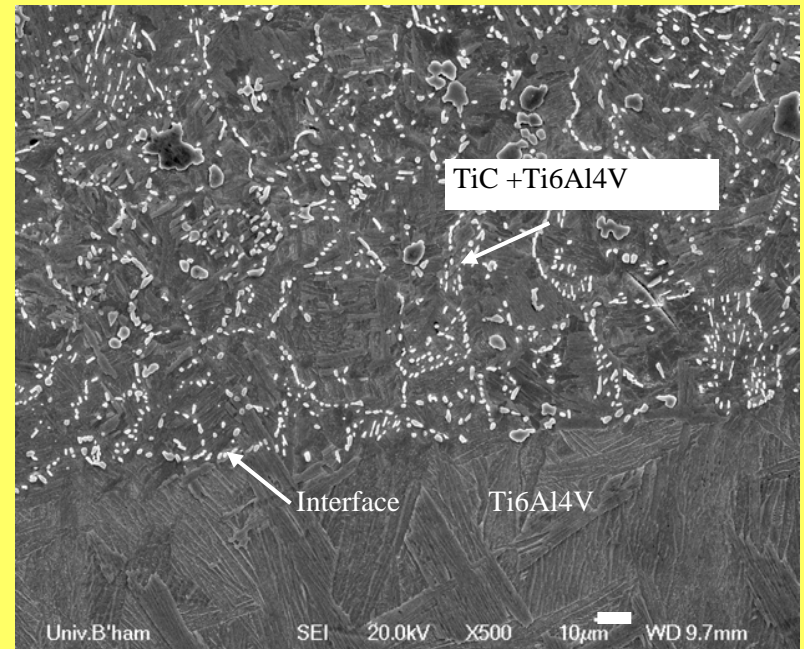
Good bonding achieved

Thermal profile/microstructure vary in the sample
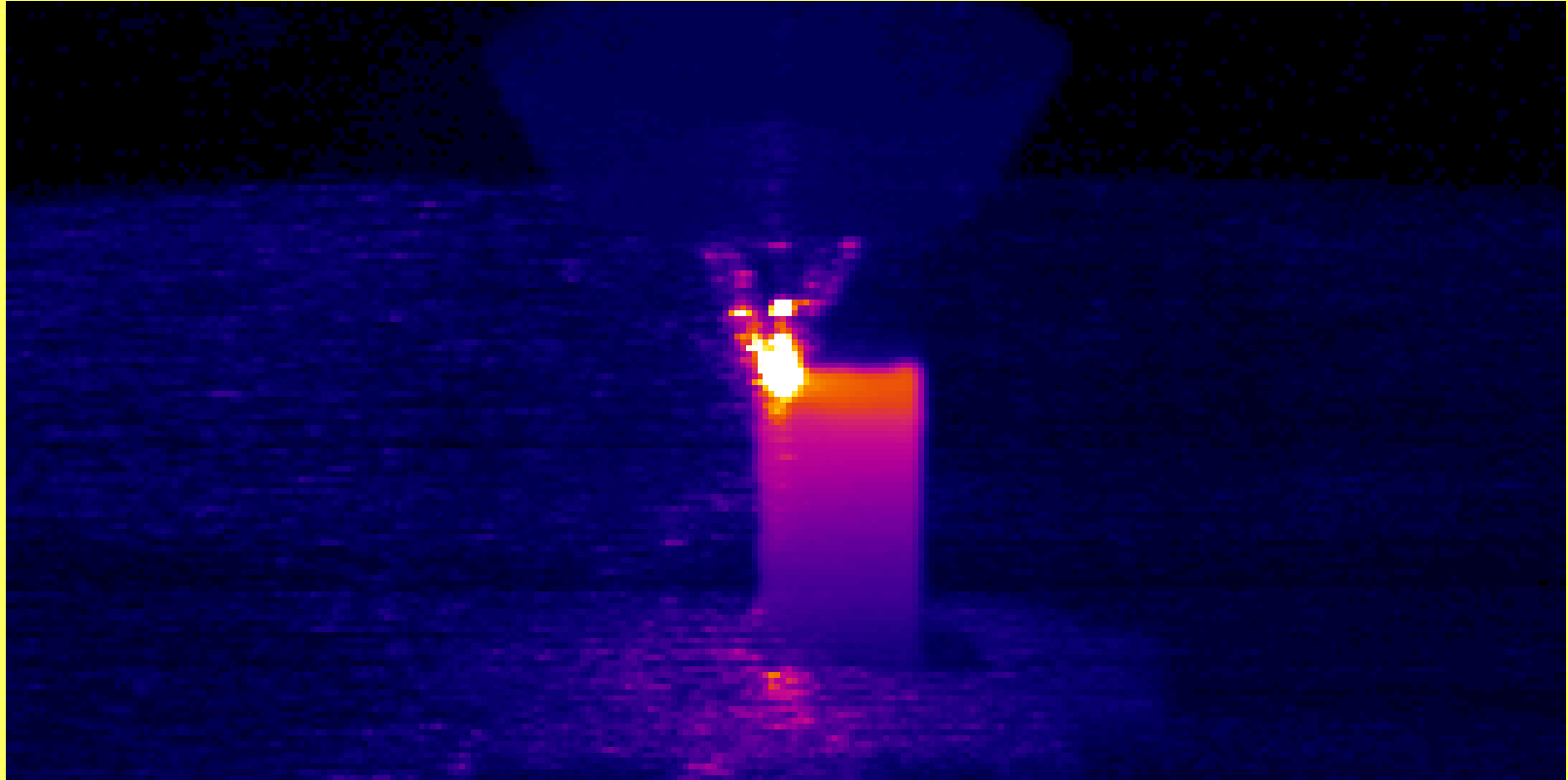
The governing equation in modelling

$$Q_{stored} = Q_{input} - Q_{conduction} - Q_{radiation} - Q_{convection} - Q_{latent}$$

$$\rho c \frac{\partial T}{\partial t} = Q_{input} - K \left(\frac{\partial^2 T}{\partial x^2} + \frac{\partial^2 T}{\partial y^2} + \frac{\partial^2 T}{\partial z^2} \right) - \varepsilon \sigma A (T^4 - T_\infty^4) - hA(T - T_\infty) - \dot{Q}_{latent}$$

T: temperature

ρ: density(kg.m^{-3})

c: specific heat capacity (J.kg^{-1}.K^{-1})

K: conductivity(W.m^{-1}.K^{-1})

t: time (s)

x, y and z are coordinates (m)

ε:emissivity

σ: Stefan-Boltzman constant 5.67 $\times 10^{-8}$ (W.m^{-2}.K^{-4})

h: convection coefficient

Q_{latent}: volumetric latent heat (W.m^{-3}) $\quad \Delta H_{1650}^{fusion} = 286 \, J g^{-1}$

$$\Delta H_{950}^{trans} = 48 \pm 10 \, J g^{-1}$$

Assumptions used in the heat transfer analysis

- Temperature-dependent thermal conductivity and heat capacity

- Preheat substrate to 180°C

- Laser absorption rate: 13-23%

- Emissivity of radiation: 0.35 (obtained experimentally)

- Convection coefficient during fabrication: 25w/mk

- Convection coefficient during cooling after fabrication (nature convection): 5w/mk

A schematic illustration of DLFed thin wall in fabrication

Moving heat source

V

Z

Y

X

Thin wall in built

Substrate

Y

Heat source

O

X
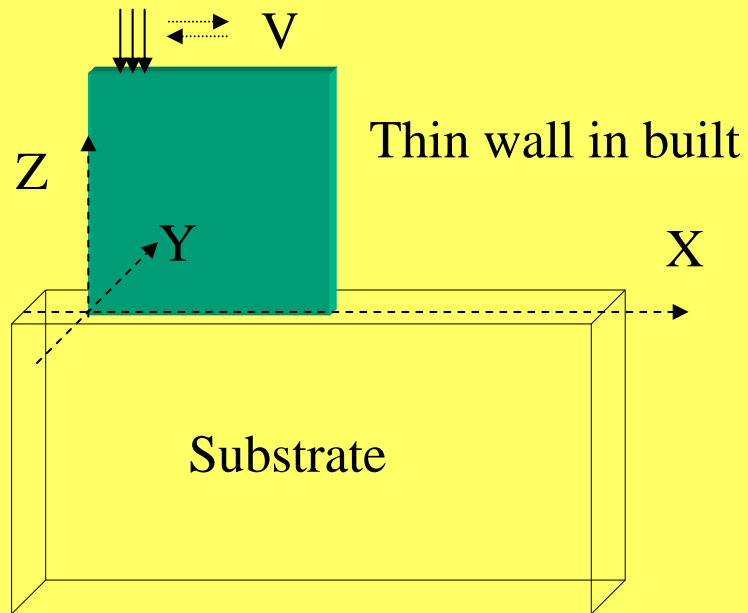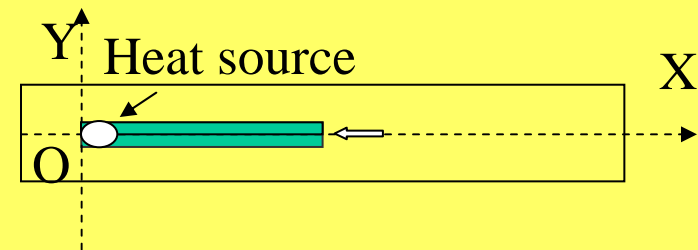
(A) Front view

(B) Top view

Mesh and configuration
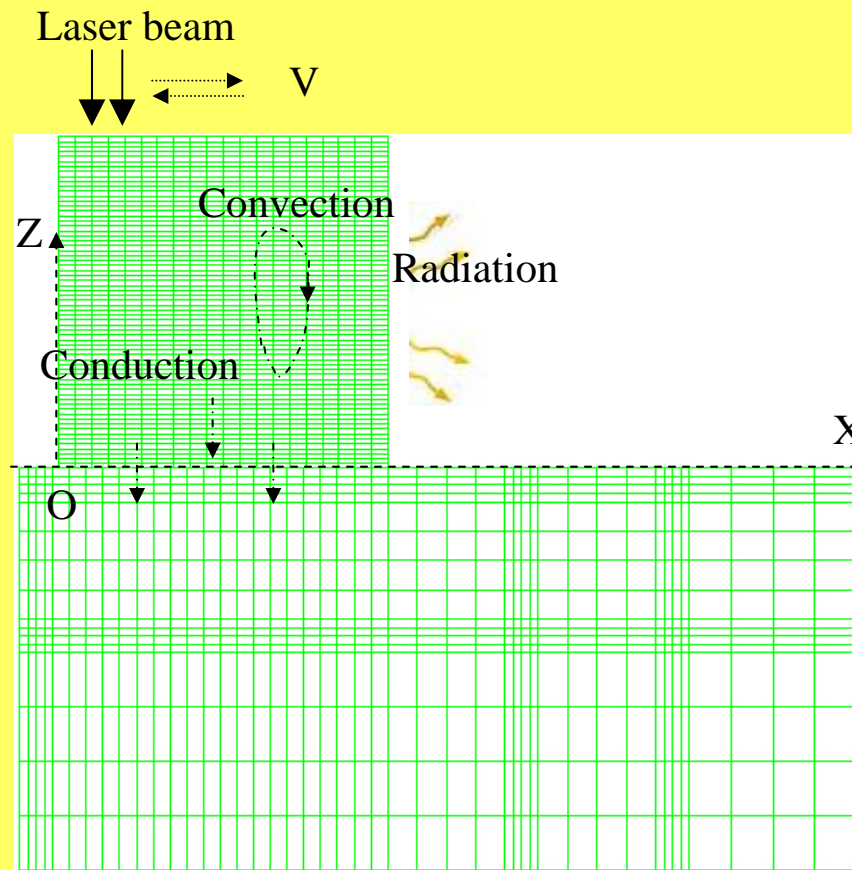
(A) Front view
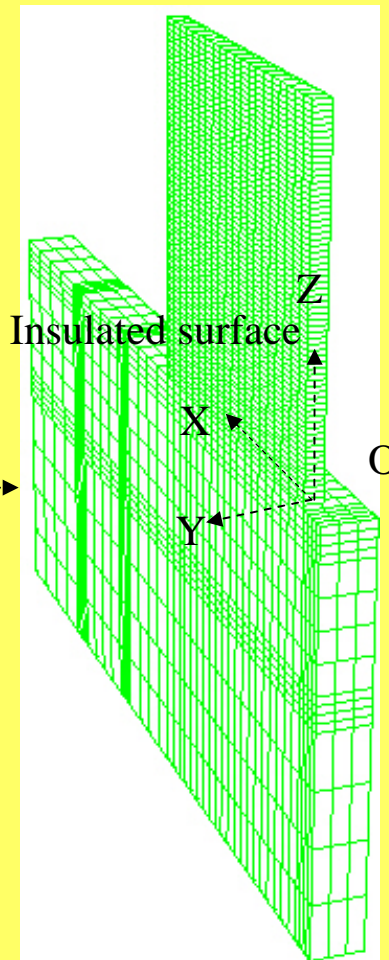
(B) Side view

Temperature Measurement Using Thermocouples
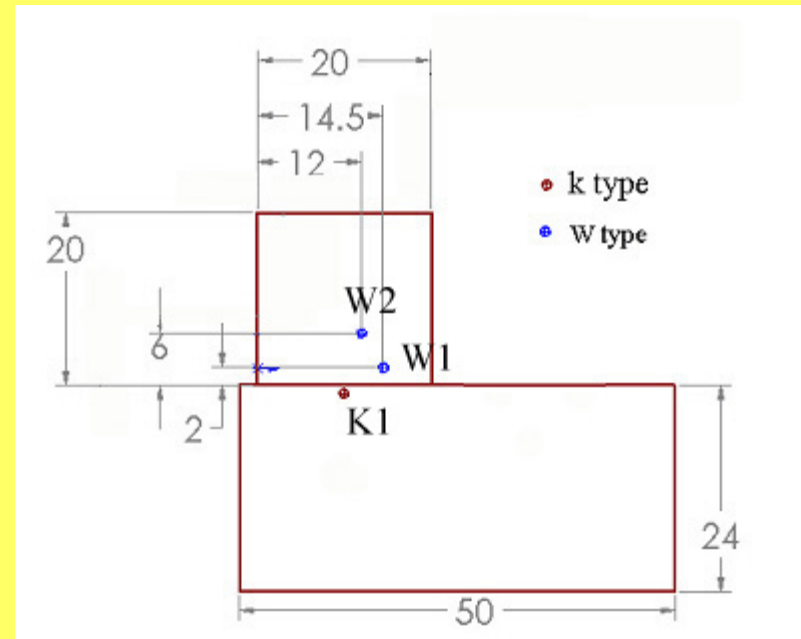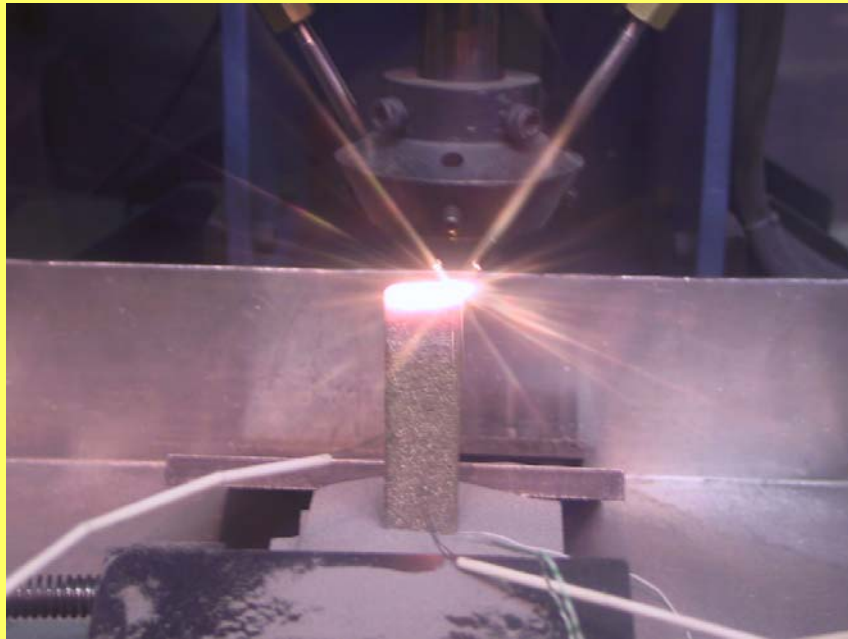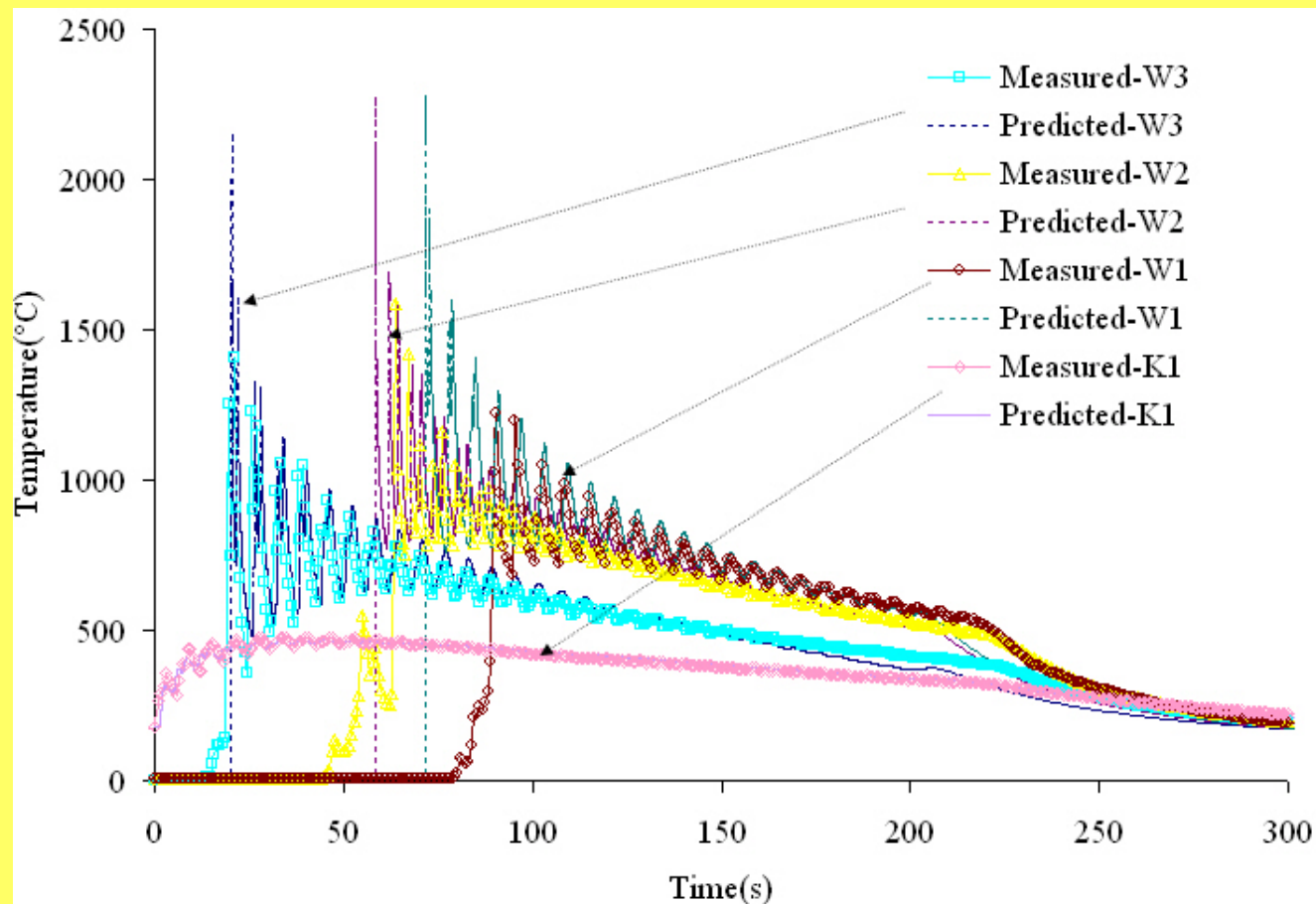
Comparison of temperatures of the predicted and the measured in DLFed Ti-6Al-4V thin wall sample built at 516w laser power, 400mm/min laser scanning speeds, 9g/min powder feed rate

The influence of location, laser power, scan speed, powder feed rate on thermal profiles has been studied , here showing only the results in the influence of location and scan speed

Heat transfer thin wall model

NT11

	+2.657e+03
	+2.331e+03
	+2.005e+03
	+1.679e+03
	+1.354e+03
	+1.028e+03
	+7.018e+02
	+3.759e+02
	+5.000e+01
	+2.500e+01

NT: Temperature (°C)

Interdisciplinary **R**esearch **C**entre **in Materials for High Performance Applications**

THE UNIVERSITY
OF BIRMINGHAM
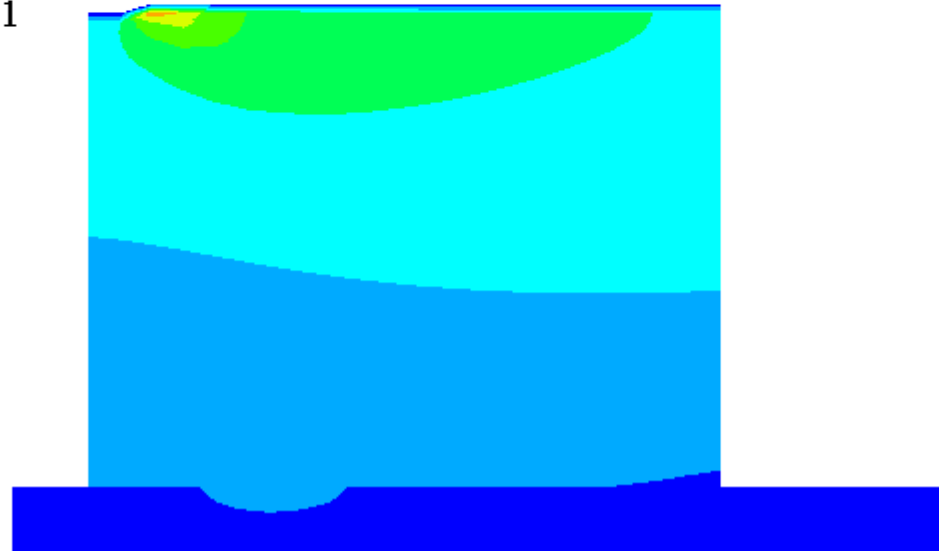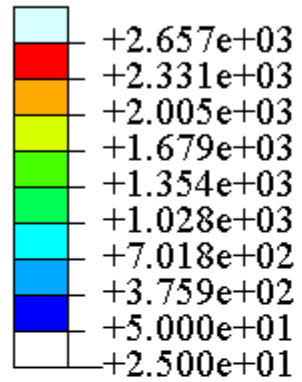
Predicted temperature profiles at a series of heights
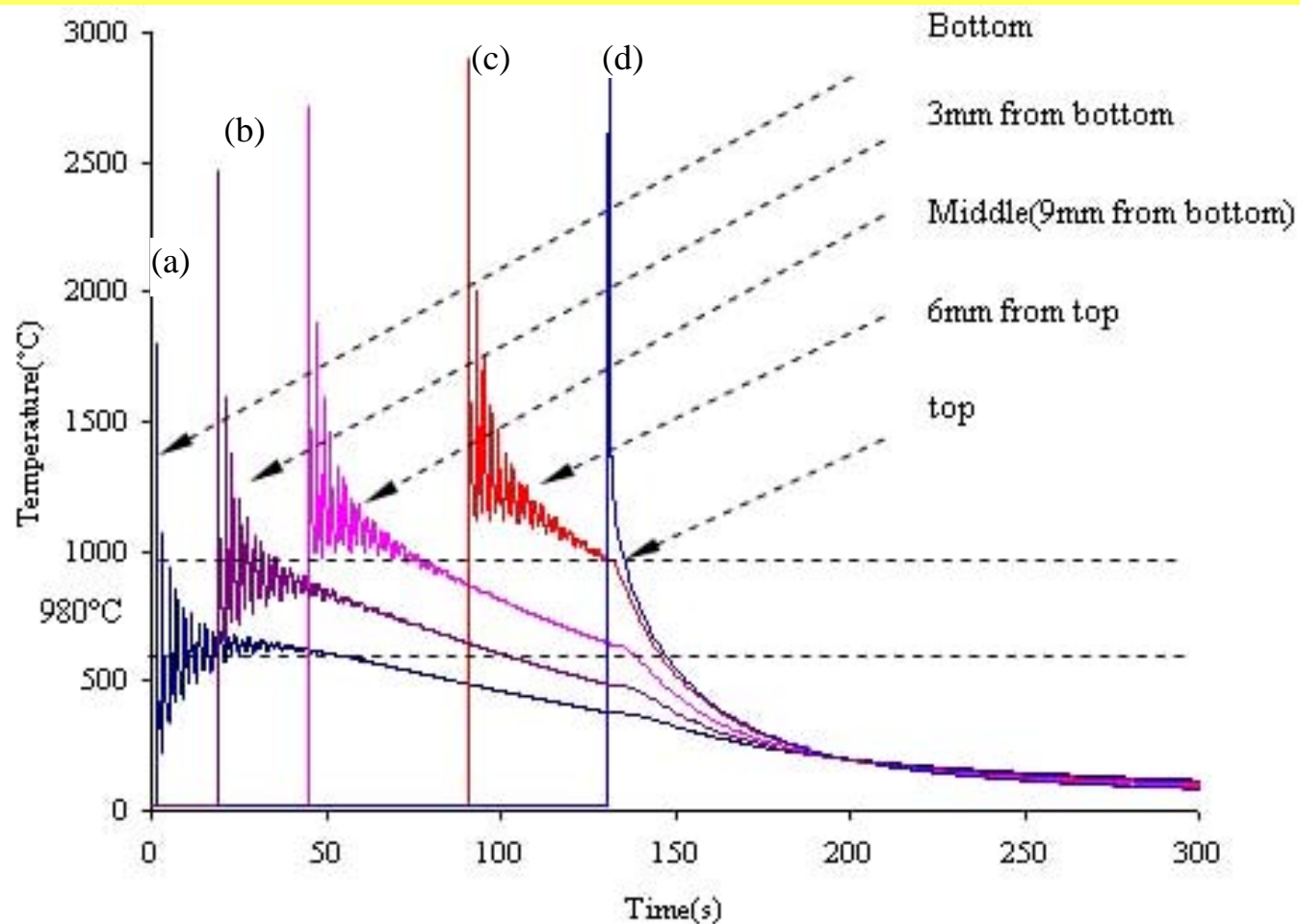
powder feed rate 18g/min

laser power 432 W

laser scanning speed 600mm/min
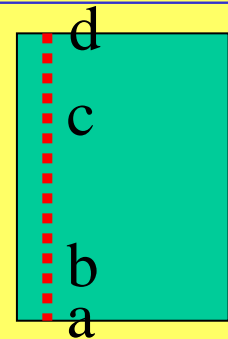
Microstructure observation

(a) 500 μm

(b)
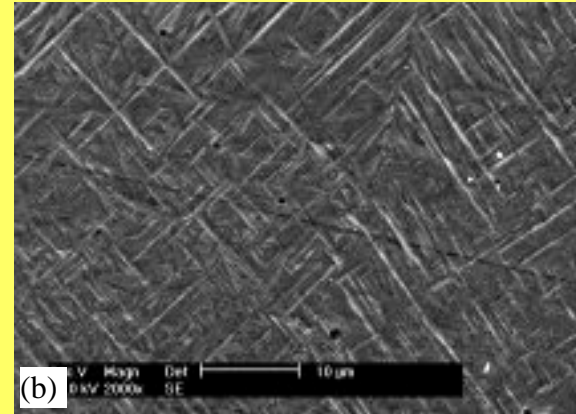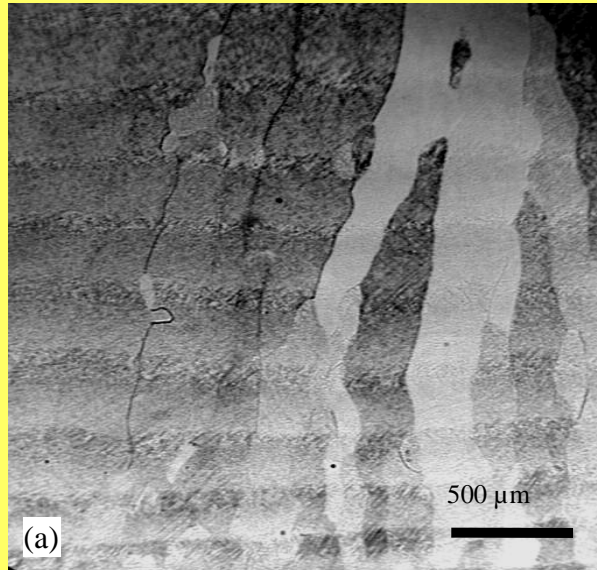
Optical micrograph showing a typical morphology of the direct laser fabricated Ti6Al4V from powder (laser power 432W, laser scan speed 600mm/min and powder feed rate18g/min); (b) SEM micrograph showing the microstructure in (a) and needle-like long laths in the microstructure
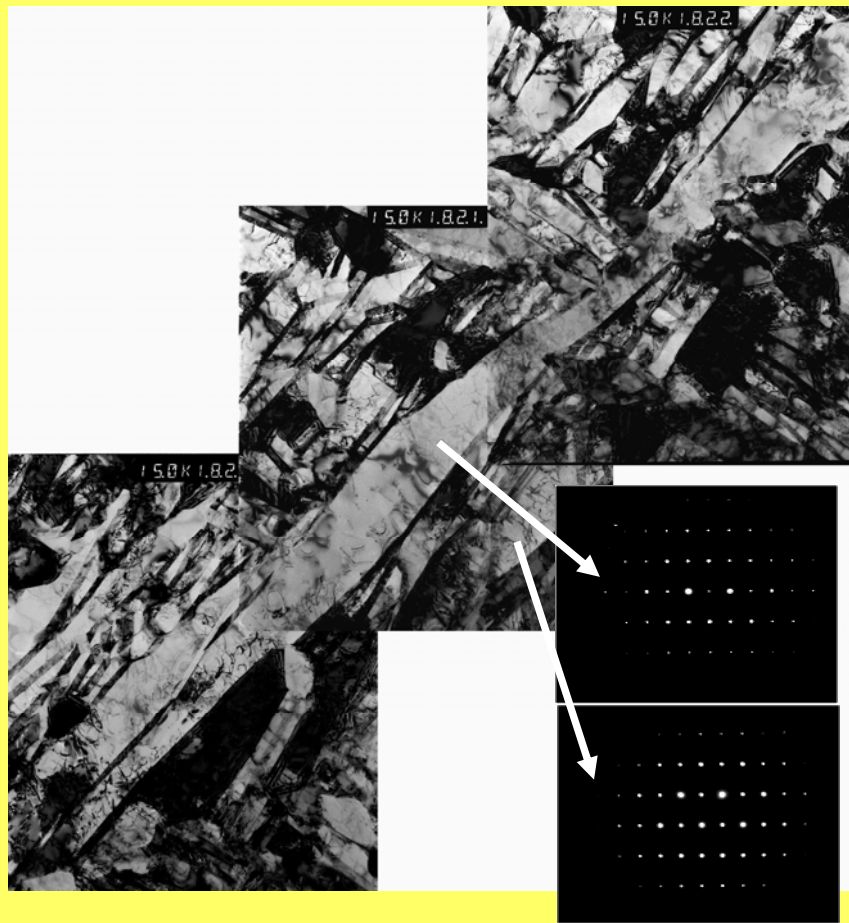
$$B = <11\overline{2}0>_{\alpha}$$

A TEM many beam image showing the long lath in the microstructure in (b) and diffraction pattern of the long lath and the short lath of the α phase in beam direction of 11-20
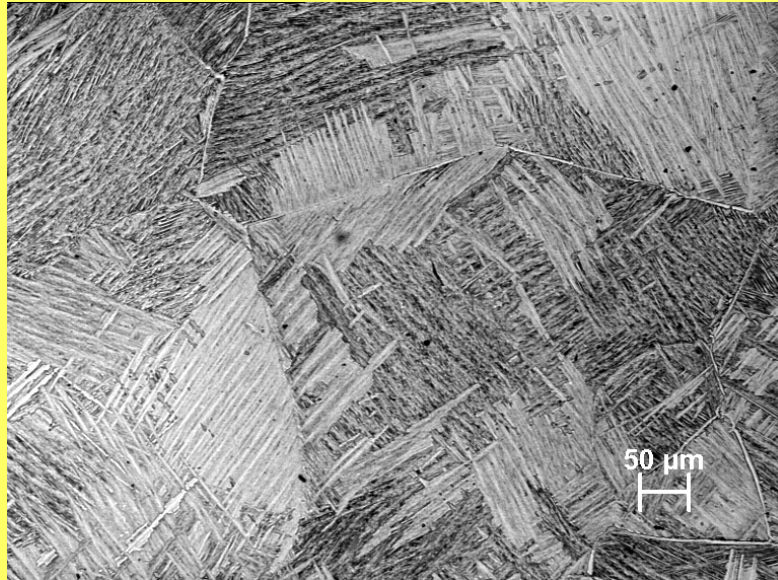
Optical micrograph showing the micorstructure of the annealed commercial Ti6Al4V and
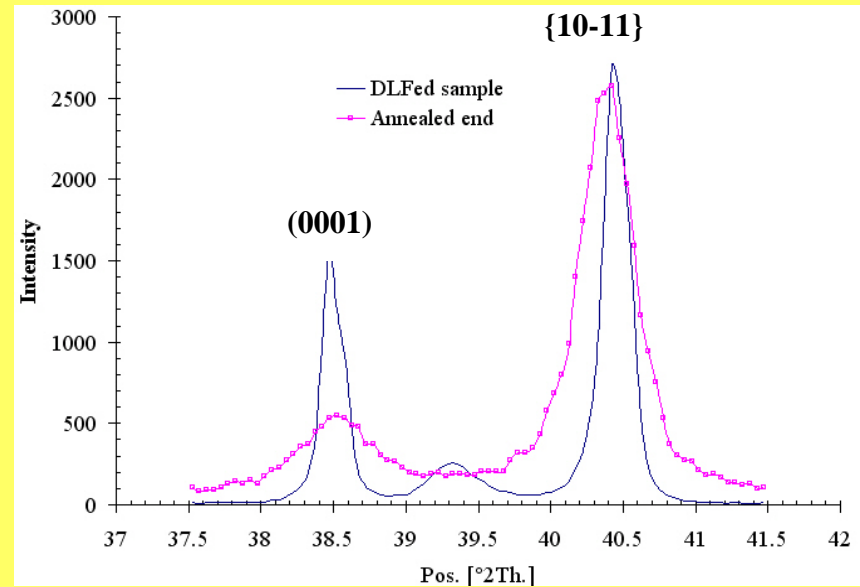
X-ray result showing the shift to a higher angle of the {10-11} peak of martensite α′ in DLFed Ti6Al4V.

Phase diagram of Ti64
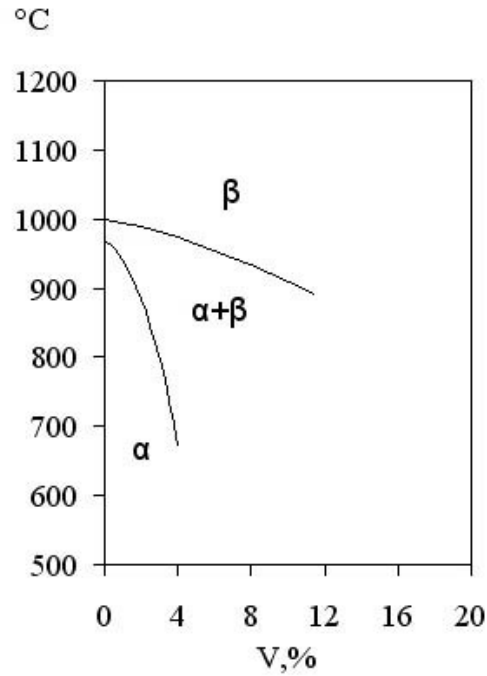
The nucleation characteristic is defined by the cooling rate within the temperature range of T_m ±20°C

(T_m: melting point)

(b)

d

c

b

a

Magn Det 10 μm
kV 2000x SE

(c) SEM 20KV X2,000 16mm 10μm

3000

(c)   (d)   Bottom

3mm from bottom

(b)   9mm from bottom

14mm from bottom

2000

(a)   top

Temperature(°C)

1000
980

600

0

0   50   100   150   200   250

Time(s)

(b) Magn Det 10 μm
2000x SE

(a) V Magn Det 10 μm
kV 2000x SE
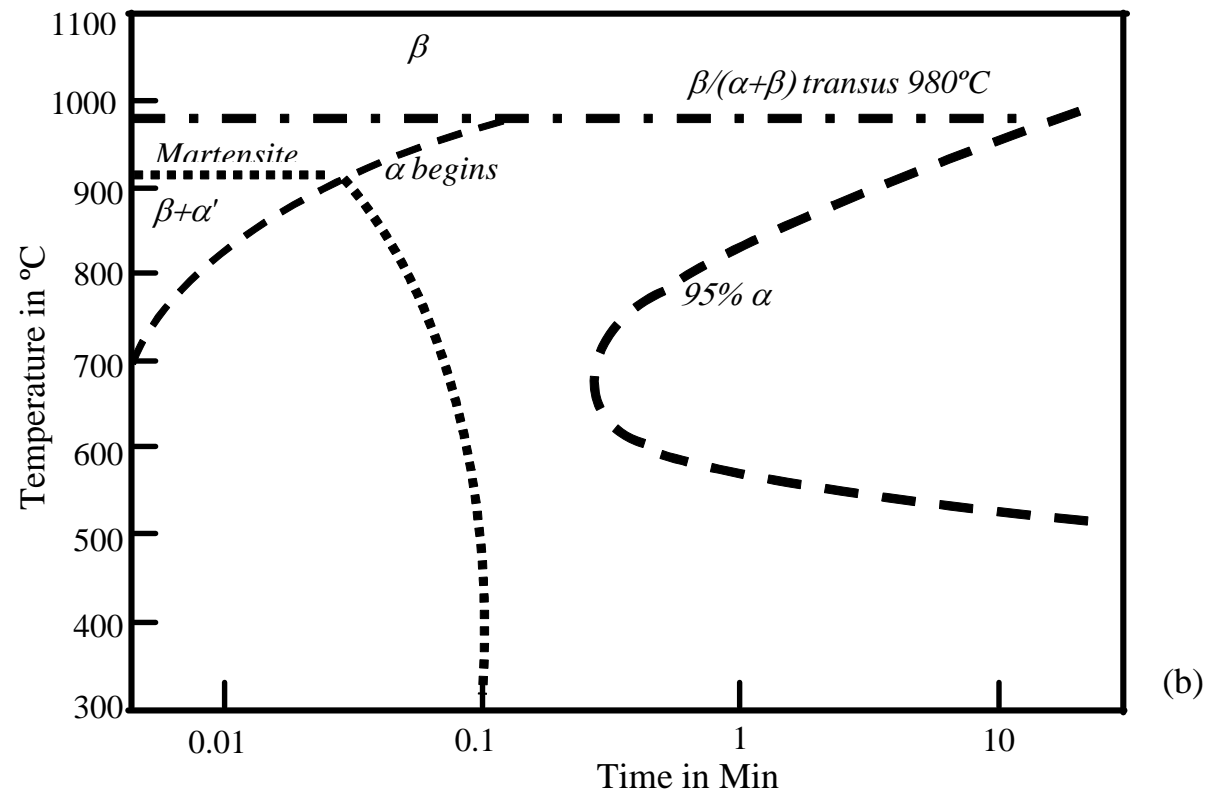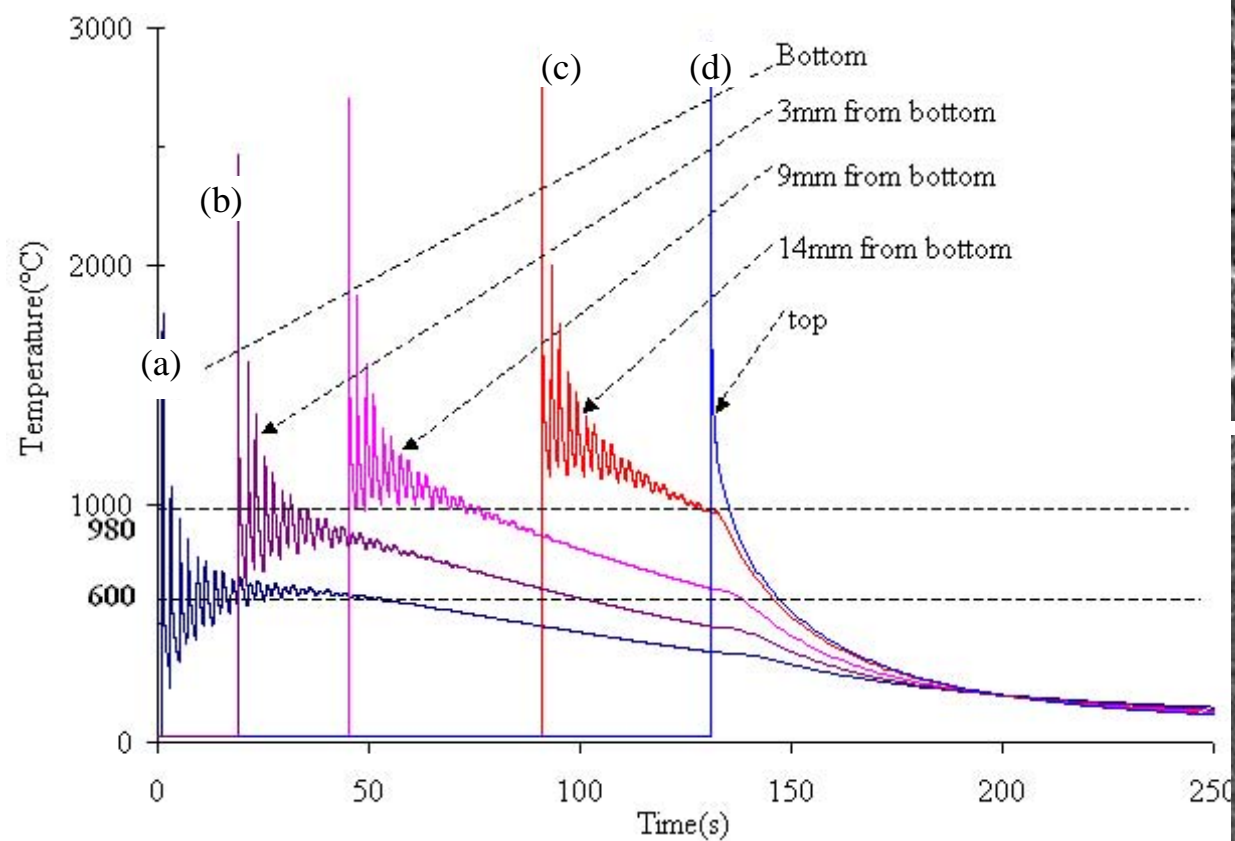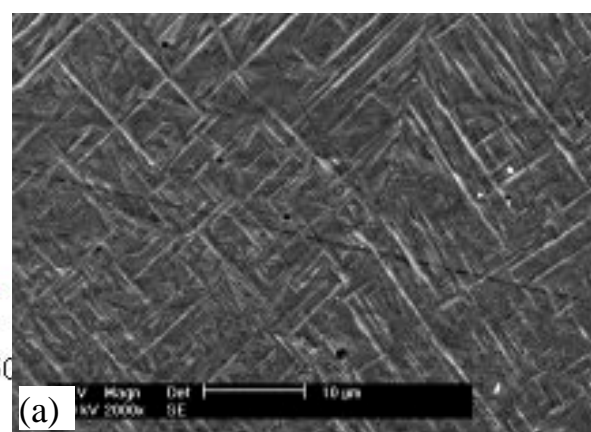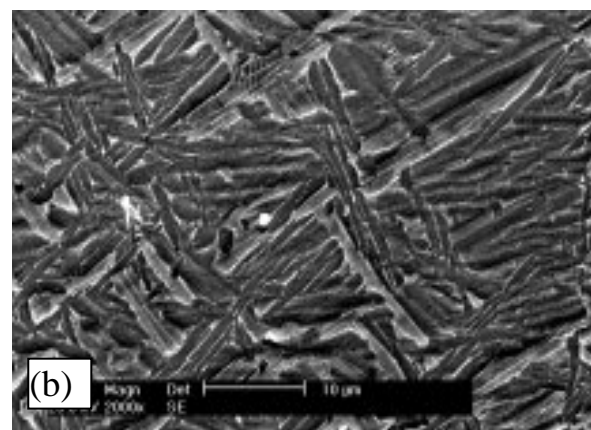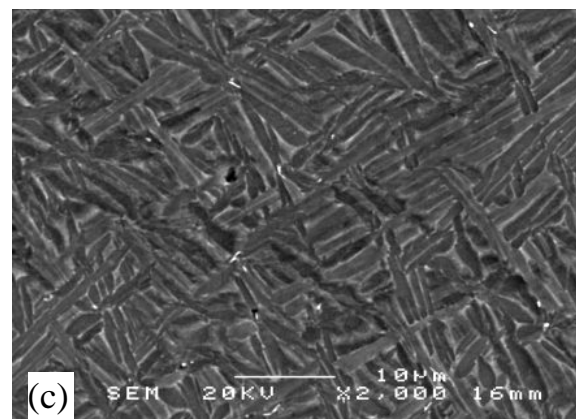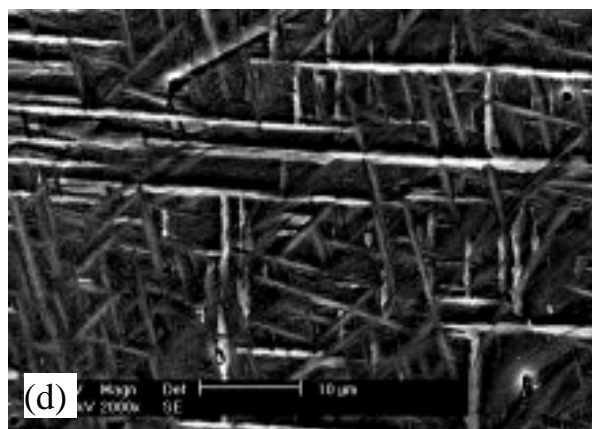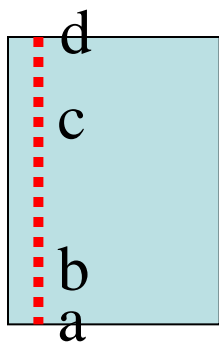
Calculated temperature profiles at the bottom of a DLFed sample at different laser scanning speeds
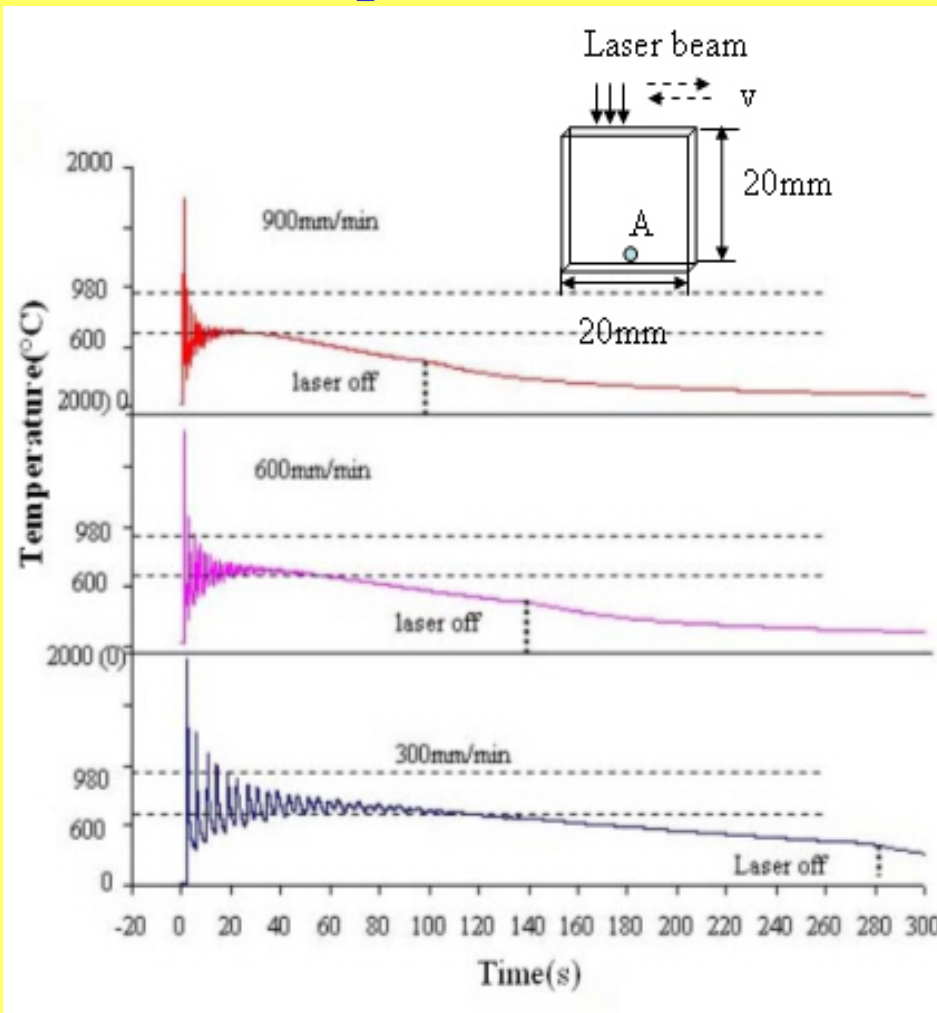
900mm/min

600mm/min

300mm/min

Influence of scan speed on molten pool
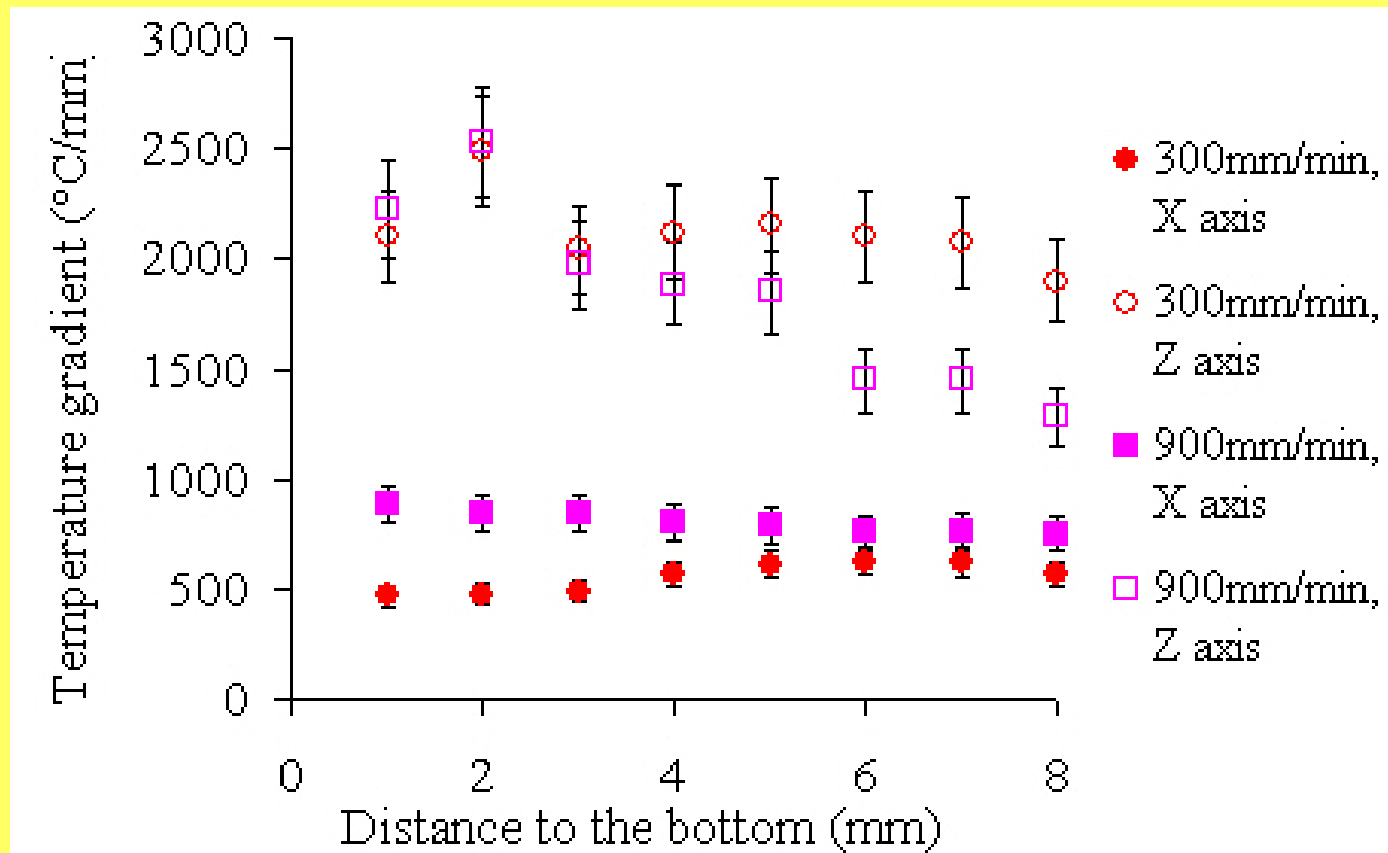## (at 3mm above bottom of the sample; 516W laser power; 8g/min powder feed rate
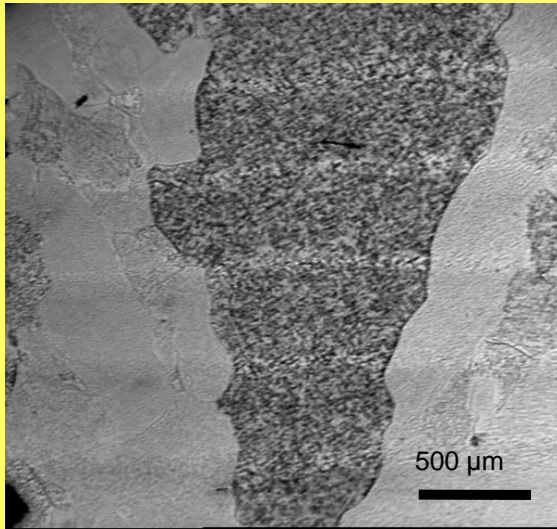
300mm/min
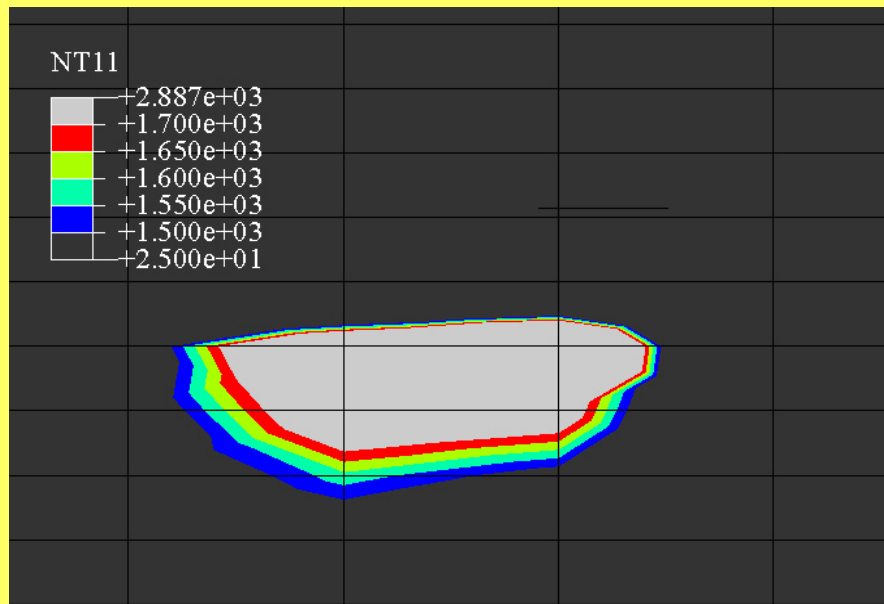
900/mm/min
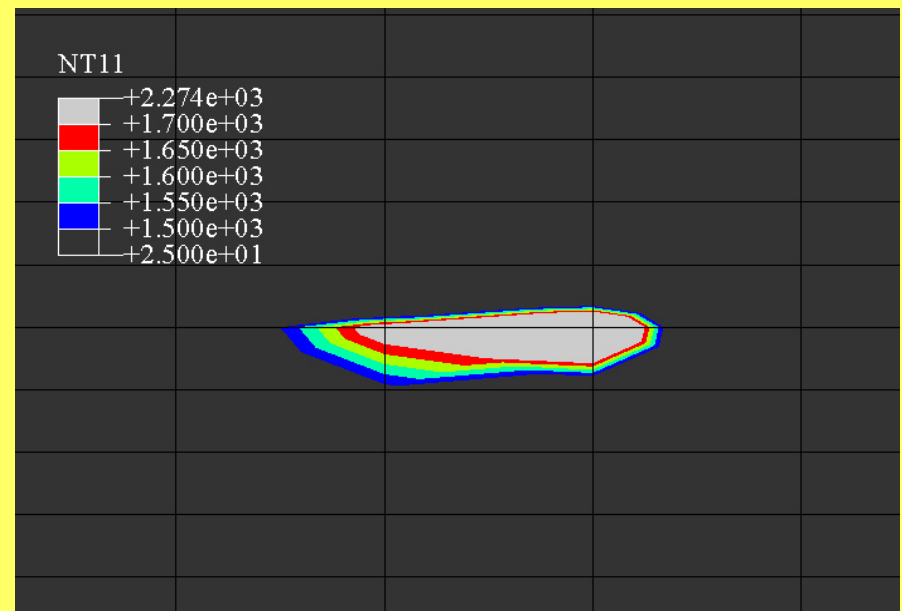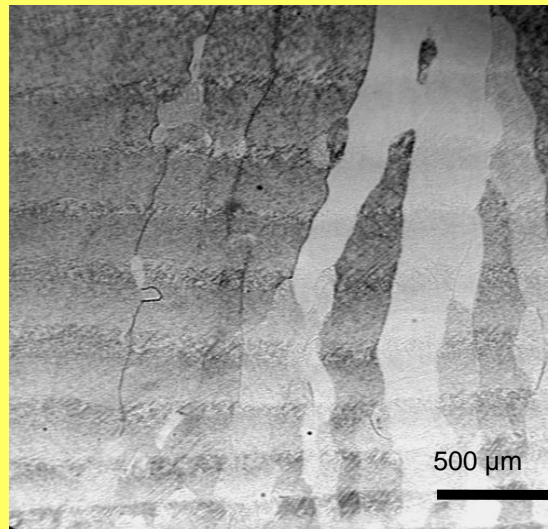
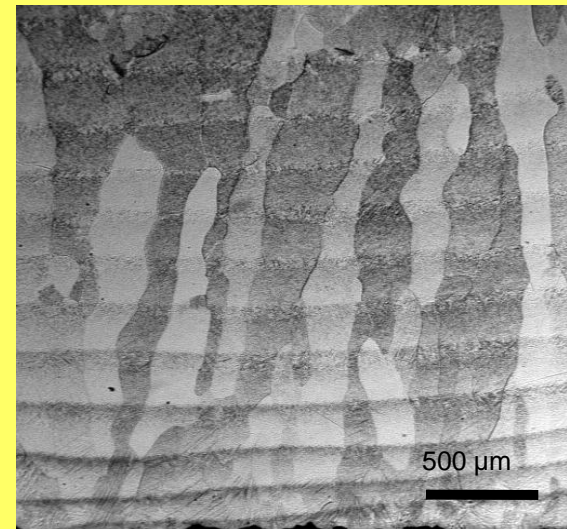# Thermal gradient at scan speeds of 300 and 900mm/min
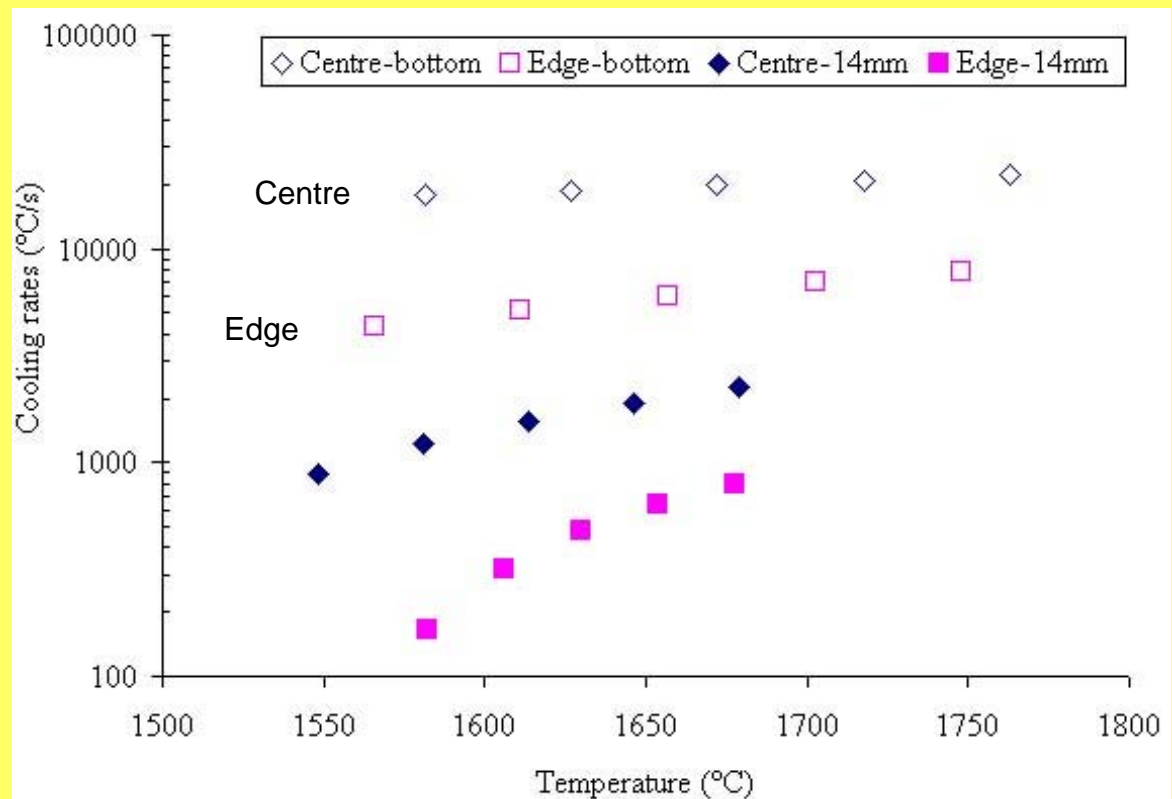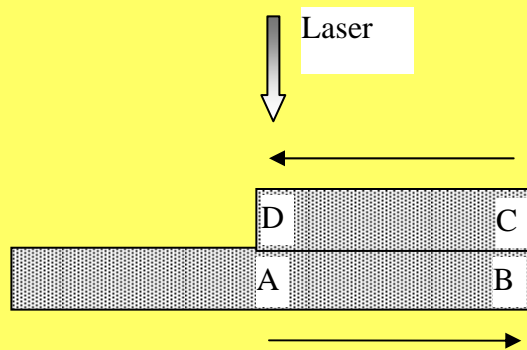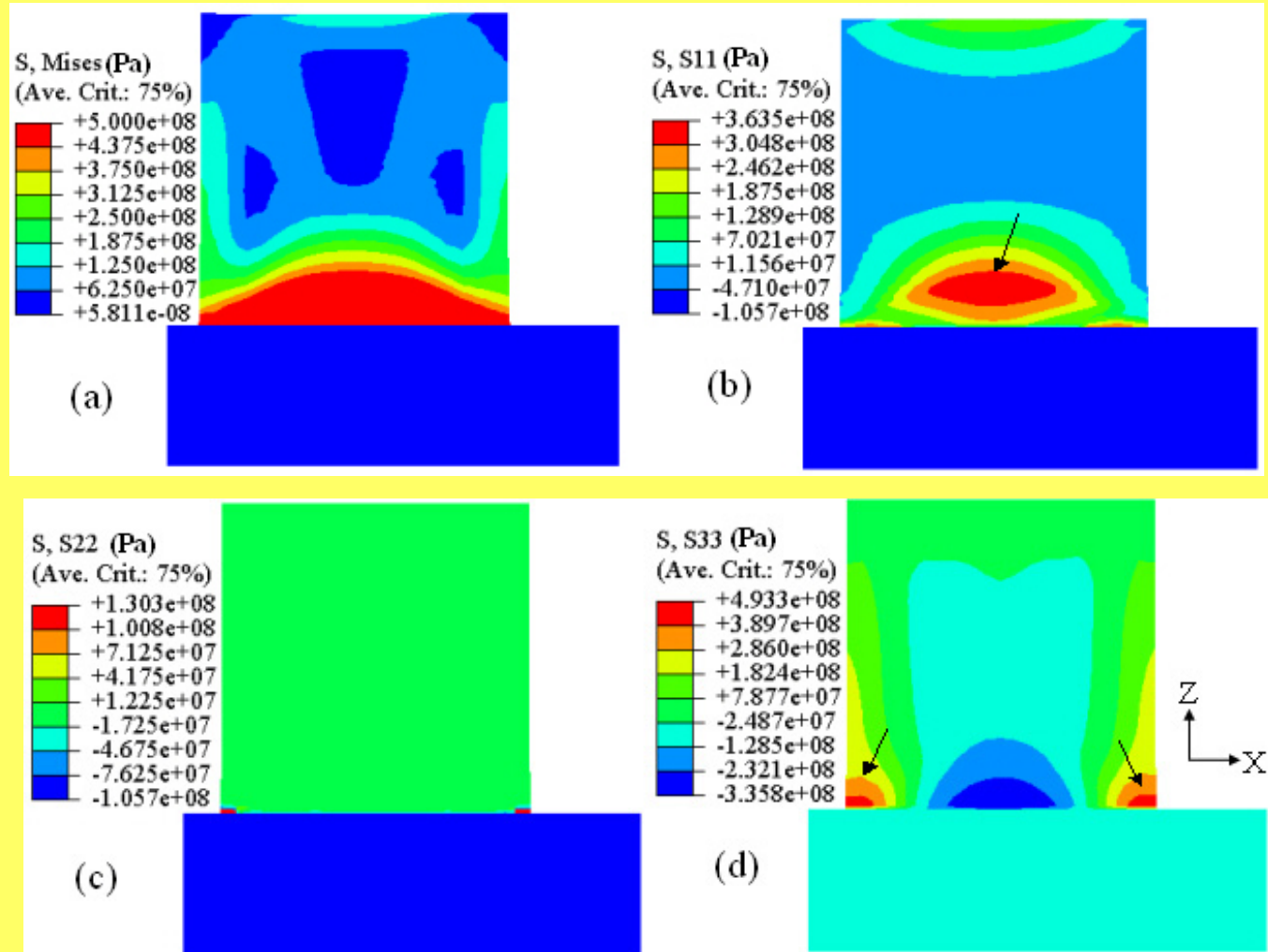
300mm/min   600mm/min   900mm/min

Optical pictures showing the columnar structure of DLFed built decreases with increasing laser scanning speed at a given powder feed rate 18g/min and a laser power of 432W. Scanning speeds are: (a) 300, (b) 600, (c) 900mm/min.

The selected grain growth of the nuclei is defined by thermal profiles as is seen in single crystal Ni alloy

Cooling rate comparison at the edge and centre

Thermal residual stress in DLFed Ti6AI4V

(a) S, Mises (Pa) (Ave. Crit.: 75%)
(b) S, S11 (Pa) (Ave. Crit.: 75%)
(c) S, S22 (Pa) (Ave. Crit.: 75%)
(d) S, S33 (Pa) (Ave. Crit.: 75%)

Interdisciplinary **R**esearch **C**entre in Materials for High Performance Applications

THE UNIVERSITY OF BIRMINGHAM

Summary

- A 3D Finite Element model has been developed for temperature history prediction in direct laser fabricated Ti6Al4V samples. The predictions match well with the measured temperature profiles

- The observed microstructures are consistent with the thermal profiles predicted or measured.

- Martensites are present in DLFed Ti6Al4V thin wall samples

- The maximum residual stress in DLFed Ti64 sample is up to 500MPa